GRIDS-TSI
Introduction to Gas Ionization Detectors

Douglas Bryman

University of British Columbia and TRIUMF

Reference: Blum and Rolandi,
http://link.springer.com/book/10.1007/978-3-540-76684-1/page/1

C. Grupen and Schwartz (2008) Particle Detectors
ajbell.web.cern.ch/ajbell/Documents/eBooks/Particle_Detectors_Grupen.pdf

Gas ionization detectors are among the principal instruments used for triggering, tracking, momentum measurements, vertex measurements, and particle identification. Also used for calorimetry, , dosimetry ….

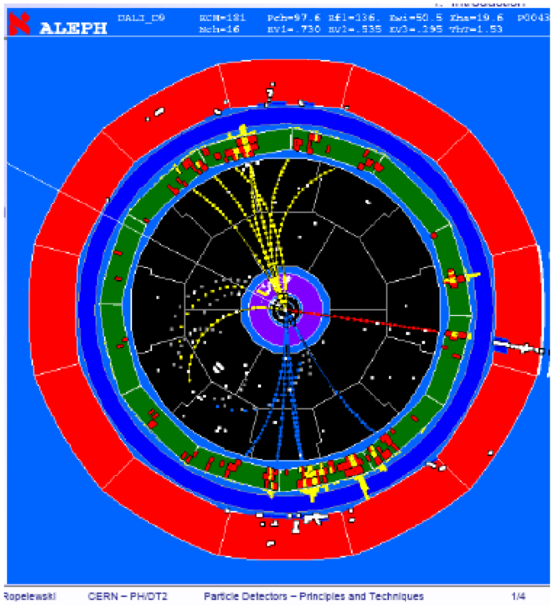

ALEPH at LEP

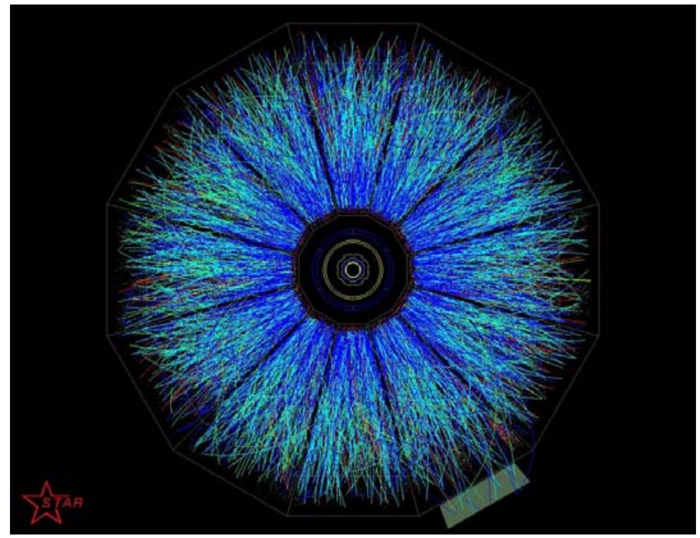

STAR TPC: Gold on Gold collision at 100+100 GeV

Gas Ionization Detectors

General types of gas ionization detectors:

- Ionization chambers (no gain)
- Avalanche chambers (gain)
  - Wires
  - Parallel plates
  - Gas electron multipliers (GEM)
  - Micro-megas

Avalanche chamber configurations:
- Geiger tubes
- Streamer chambers
- Drift chambers
- Multi-wire proportional chambers (MWPC)
- Time projection chambers
- Time expansion chambers
- …

Other gas-based detectors:
- Cerenkov
- Transition radiation
- Scintillation

Outline

1. Ionization, energy loss, drift, and diffusion
2. Ionization chambers
3. Proportional and avalanche chambers
4. Drift chambers
5. Microstructure avalanche chambers
6. Summary

1. Ionization, energy loss, drift, and diffusion

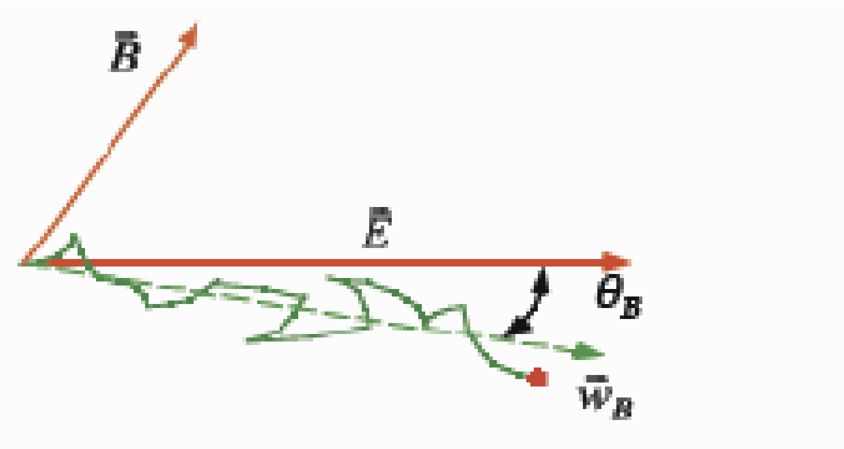

Ionization Energy Loss - source of primary ionization

Stopping Power
(dE/dx) vs βγ
(Momentum)

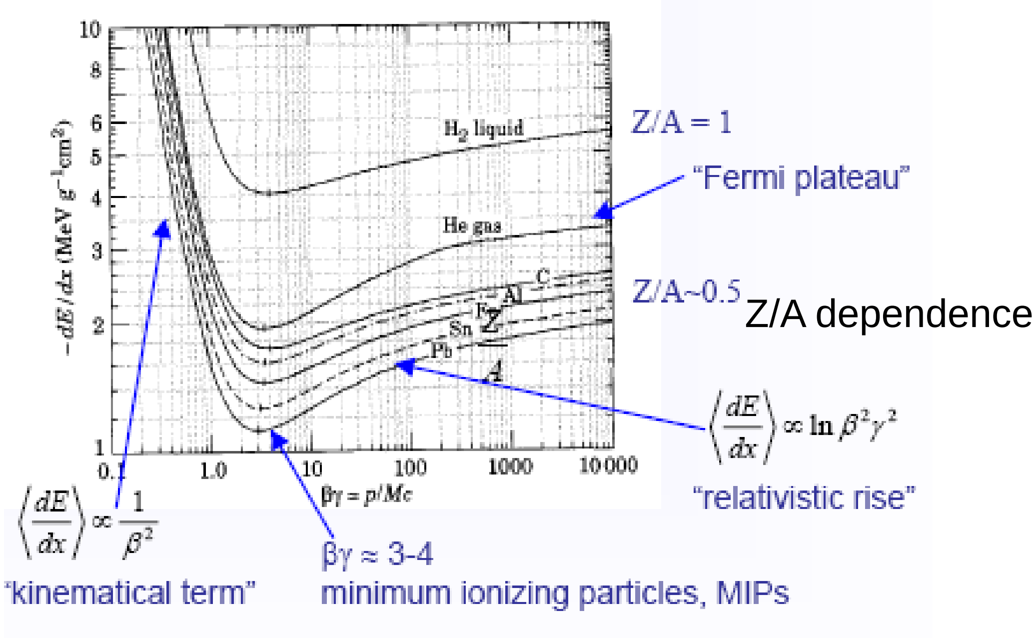

Particle	MIP region	$\frac{dE}{dx}_{mip}$ $MeV/g/cm^2$	Material
μ	$300MeV/c$	4.12	$H_2(liq./gas)$
π	$400MeV/c$	1.95	CH (scintillator)
p	$3GeV/c$	1.51	$Ar(liq./gas)$
		1.13	Pb

SEE: The Review of particle Physics, Journal of Physics G33,1 (2006)
http://pdg.lbl.gov/

Muon Stopping Power (dE/dx) vs Momentum

PDG

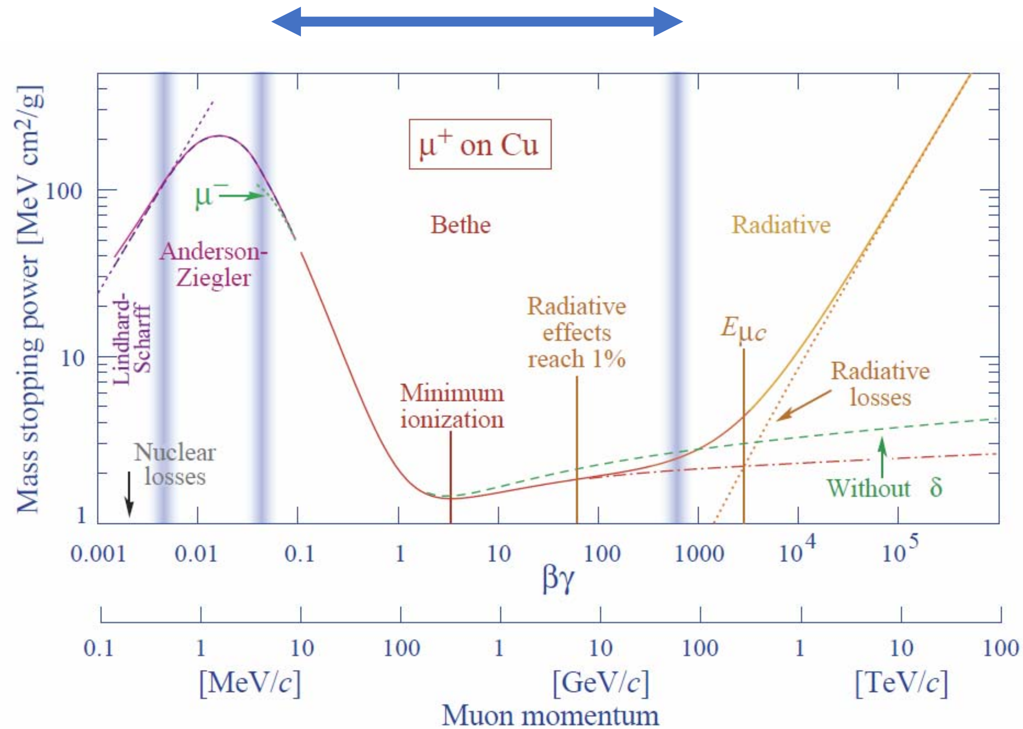

Fig. 33.1: Mass stopping power ($= \langle -dE/dx \rangle$) for positive muons in copper as a function of $\beta\gamma = p/Mc$ over nine orders of magnitude in momentum (12 orders of magnitude in kinetic energy). Solid curves indicate the total stopping power. Data below the break at $\beta\gamma \approx 0.1$ are taken from ICRU 49 [4], and data at higher energies are from Ref. 5. Vertical bands indicate boundaries between different approximations discussed in the text. The short dotted lines labeled "μ^-" illustrate the "Barkas effect," the dependence of stopping power on projectile charge at very low energies [6]. dE/dx in the radiative region is not simply a function of β.

δ Rays

Energetic electrons (>few keV) produced in collisions are the source of secondary ionization and clusters.

Number of δ rays ($E_0 \ll E_{max}$):

$$N_\delta(E > E_0) = x \int_{E_0}^{E_{max}} \Phi_{col} dE'$$

$$= \frac{2\pi N_A z^2 e^4 Z x}{\beta^2 m_e^2 A E_0} \equiv \frac{W}{E_0}$$

$N_A = 6x10^{23}$ $\quad W = \frac{0.15 Z z^2 x}{\beta^2 A}[MeV]$

Example: $\beta \sim 1,\ \frac{Z}{A} = 0.5,\ x = 0.2\frac{g}{cm^2} \rightarrow W = 15keV$

$$N_\delta(E > 15keV) = \frac{W}{15} = 1$$

Z,A= atomic numbers of molecules
z= charge of particle
x= thickness of gas (gm/cm^2)
m_e=electron mass
β=v/c = incident particle velocity/c

Ionization Statistics

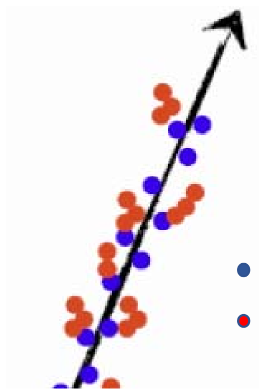

- Primary
- Secondary

Parameters :

Ionization Energy	E_i
Average Energy/ion pair	$W_i \sim 30$ eV for gases
Average no. primaries/cm	n_p
Average no. pairs/cm	$n_T \sim 100/3keV \ (\sim 2-6 \ \ n_p)$

Z vs. n_p

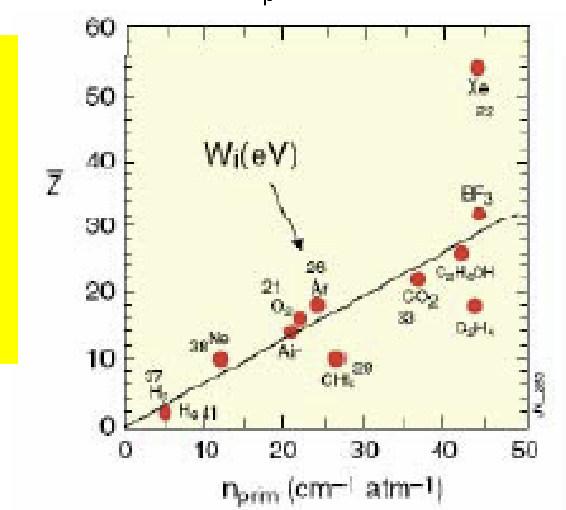

Production of primary e/ion pairs has a Poisson distribution:

$$P(n_p, \langle n_p \rangle) = \frac{\langle n_p \rangle^{n_p} e^{-\langle n_p \rangle}}{n_p!}$$

$$\lambda = \text{mean free path} = \frac{1}{n_e \sigma}, \ \langle n_p \rangle = \frac{L}{\lambda}$$

Table for most common gases

($E_i = I_o$)

Gas	ρ (g/cm³) (STP)	I_0 (eV)	W_i (eV)	dE/dx ($MeVg^{-1}cm^2$)	n_p (cm^{-1})	n_t (cm^{-1})
H_2	$8.38 \cdot 10^{-5}$	15.4	37	4.03	5.2	9.2
He	$1.66 \cdot 10^{-4}$	24.6	41	1.94	5.9	7.8
N_2	$1.17 \cdot 10^{-3}$	15.5	35	1.68	(10)	56
Ne	$8.39 \cdot 10^{-4}$	21.6	36	1.68	12	39
Ar	$1.66 \cdot 10^{-3}$	15.8	26	1.47	29.4	94
Kr	$3.49 \cdot 10^{-3}$	14.0	24	1.32	(22)	192
Xe	$5.49 \cdot 10^{-3}$	12.1	22	1.23	44	307
CO_2	$1.86 \cdot 10^{-3}$	13.7	33	1.62	(34)	91
CH_4	$6.70 \cdot 10^{-4}$	13.1	28	2.21	16	53
C_4H_{10}	$2.42 \cdot 10^{-3}$	10.8	23	1.86	(46)	195

Quelle: K. Kleinknecht, *Detektoren für Teilchenstrahlung*, B.G. Teubner, 1992

Drift and Diffusion of Electrons in Gases

Electric field E=0

Elastic collision,
recombination, diffusion….

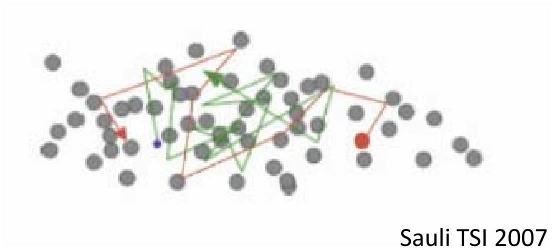

Sauli TSI 2007

Electric field E>0

Net motion of ions and
electrons; longitudinal and
transvers diffusion

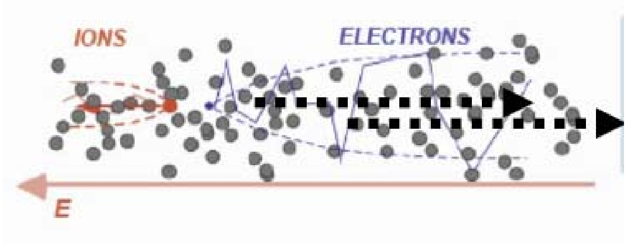

Electron and ion clouds drift at constant velocity, diffuse and (in some materials, but not noble gases) are diminished by attachment.

Drift of Electrons in Gases

From classical kinetic theory of gases, in the presence of an electric field **E** at pressure P, electrons are accelerated:

$$\text{Drift velocity } w \sim \frac{eE}{m}\left\langle \frac{\lambda}{v} \right\rangle = \frac{eE}{m}\tau$$

$v =$ instantaneous velocity

$\lambda =$ mean free path $(\alpha\, \mathrm{P}^{-1})$

$\tau =$ mean time between collisions

Electron Drift velocity $w_e = \mu_e E \sim cm/\mu s$

$$\mu = \frac{e\tau}{m_e} = \text{Mobility}$$

Ion Drift velocity $w_I = \mu_I E \sim cm/ms$

$$\lambda(\varepsilon) \equiv \frac{1}{N\sigma(\varepsilon)} = \text{Mean Free Path } [cm]$$

Density $N[\frac{at}{cm^3}]$, Collision cross section $\sigma\left[cm^2\right]$

DRIFT AND DIFFUSION OF ELECTRONS IN GASES

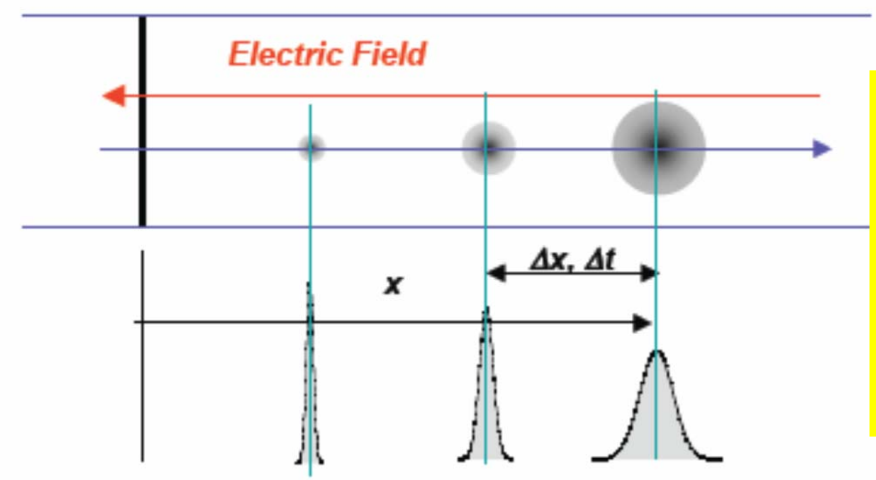

Gaussian Diffusion: $\frac{dN}{N} = \frac{1}{\sqrt{4\pi Dt}} e^{-(\frac{x^2}{4Dt})} dx$

Linear Diffusion width $\sigma(x) = \sqrt{2Dt} = \sqrt{2D\frac{x}{w}}$

D = Diffusion coefficient

In the presence of electric fields, Longitudinal diffusion D_L is different from Transverse diffusion D_T

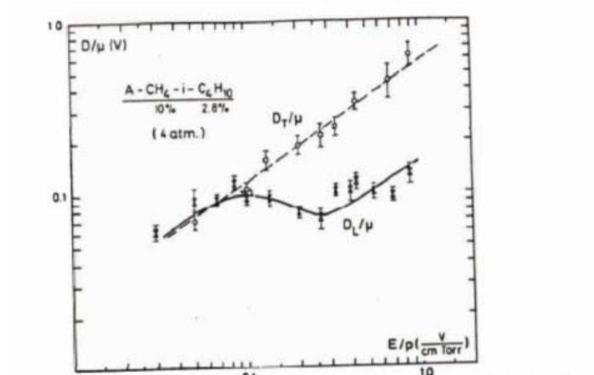

Figure 18: *Longitudinal and transverse diffusion coefficients for a Ar-CH₄-C₄H₁₀ gas mixture as function of the electric field [60].*

Drift and Diffusion in Gases

Molecular cross sections are complex and material dependent; drift velocity, diffusion properties vary :

- Some gases have low diffusion e.g. CO_2 “cool” gas
- Some have larger diffusion e.g. Ar
- (These properties also depend on the presence of magnetic fields)

Example: Ramsaur-Townsend effect in Ar

A minimum in the electron-Atomic cross section at

$\sigma(\varepsilon)$ occurs at $\varepsilon \sim \frac{1}{3} eV$

Big effect in Ar and Ar-mixtures.

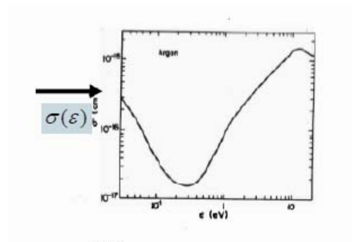

Drift Velocity vs E for Ar CH_4 mixtures

Electron drift velocity vs. Electric field for mixtures of Ar+methane

$w[\frac{cm}{\mu s}]$

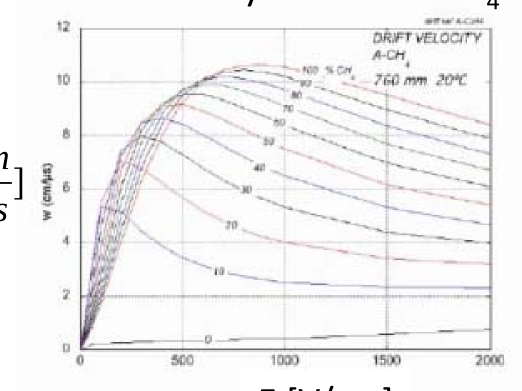

E [V/cm]

Typical value $\rightarrow w\sim 5\frac{cm}{\mu s}$

Drift and Diffusion in the Presence of Electric and Magnetic Fields

Drift velocity **w** in the presence of electric and magnetic fields:

$$\mathbf{w} = \frac{e}{m_e}\frac{\tau}{1+\omega^2\tau^2}\left[\mathbf{E} + \omega\tau\frac{\mathbf{E}x\mathbf{B}}{B} + \omega^2\tau^2\frac{\mathbf{B}(\mathbf{E}\bullet\mathbf{B})}{B^2}\right]$$

$\tau =$ mean time between collisions

$\omega =$ cyclotron frequency $= \frac{eB}{m_e}$

$\mathbf{E} \perp \mathbf{B}$

Drift at angle $\alpha_{H:}$ $\tan(\alpha_H) = \omega\tau$

Drift velocity $\mathrm{w}_H = \frac{w(0)}{\sqrt{1+\omega^2\tau^2}}$

$\mathbf{E} \parallel \mathbf{B}$

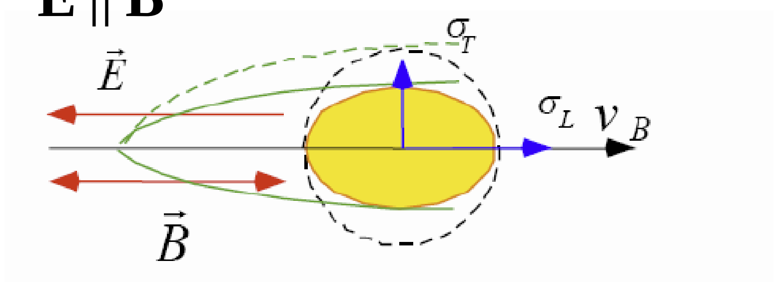

Transverse Diffusion Suppressed $\frac{D_T(B)}{D(0)} = \frac{1}{\sqrt{1+\omega^2\tau^2}}$

Principle of the Time Projecton Chamber

2. Gas Ionization Chambers

Example usages for gas ionization chambers:
- X-ray energy measurements e.g. keV region
- α energy, position measurements
- Fission fragments

Planar Geometry

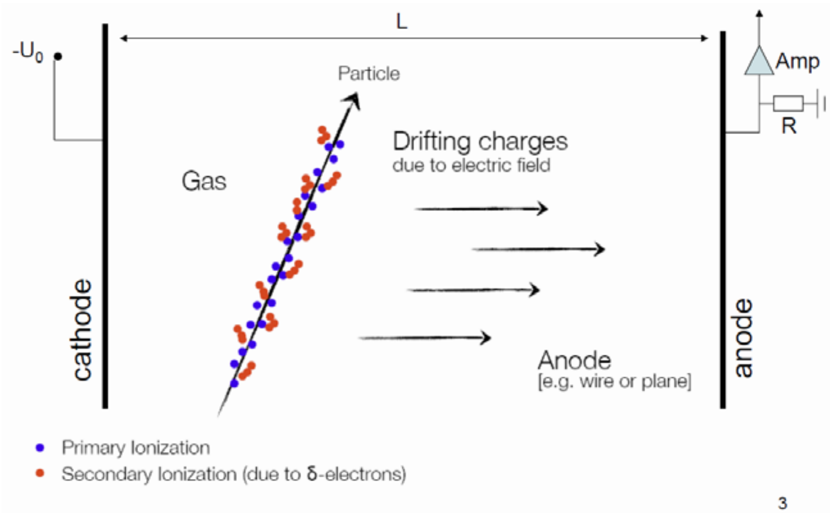

- ***Electron signal on anode depends on position of ionization or drift time.***

One solution: Frisch Grid:

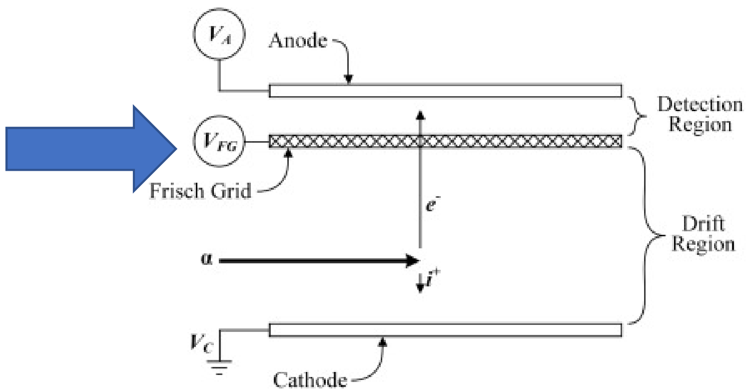

Eliminates position dependence of signal on anode for ionization between cathode and grid.

Gas Ionization Chambers–Cylindrical Geometry

Ionization at r_0

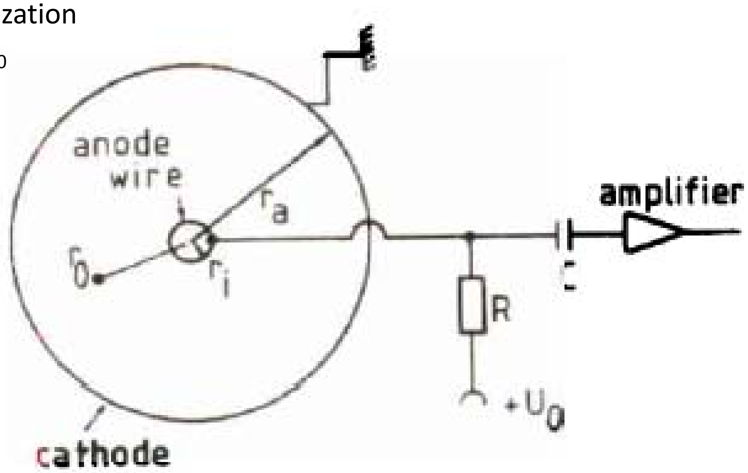

Grupen

Solve the LaPlace equation: $\nabla^2 V = 0$

$$V(r) = V_0 \frac{\ln\left(\frac{r_0}{r_a}\right)}{\ln\left(\frac{r_i}{r_a}\right)}$$

Field $\quad \mathbf{E}(r) = -\nabla V$

$$\left|\mathbf{E}(r)\right| = \frac{V_0}{r_0 \ln\left(\frac{r_a}{r_i}\right)} \quad \alpha \quad \frac{1}{r_0}$$

Electric field and drift velocity are not constant.

Charge Collected in an Ion Chamber

For a m.i.p., ~120 ion pairs in 1 cm at STP
in a cylindrical chamber with capacitance 10pf,
what is the voltage change -- is it measurable?

$$V = \frac{Ne}{C} = \frac{(120)1.6x10^{-19}}{10\,pf}$$

$$\approx 2\mu V$$

This is gernerally too small to detect:

Need GAIN to increase the signal.

Gas Gain: M

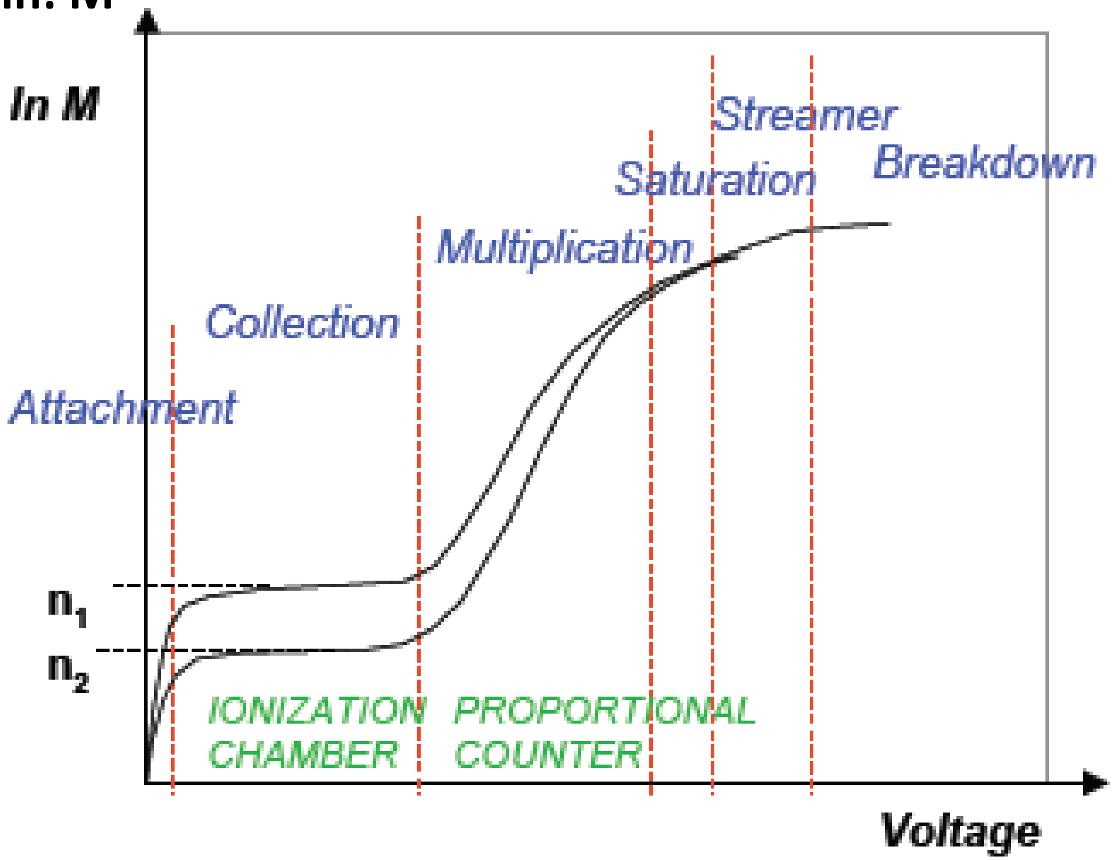

ln M
Streamer
Breakdown
Saturation
Multiplication
Collection
Attachment
n1
n2
IONIZATION
CHAMBER
PROPORTIONAL
COUNTER
Voltage

3. Proportional and Avalanche Chambers
Gas Amplification by Ionization

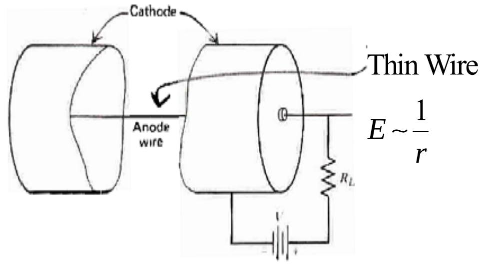

Grupen

At high electric fields in gases, excitation and charge multiplication occurs.

Complex secondary processes in mixtures:

Radiative recombination:	$A^{+} + B \rightarrow AB + h\nu$
Radiative capture:	$e + M \rightarrow M^{-} + h\nu$
Dissociative capture:	$e + AB \rightarrow AB^{-} \rightarrow A + B^{-}$
Three-body collision:	$e + A = B \rightarrow A^{-} + B$
Dimer formation and decay:	$A^{*} + A \rightarrow A^{*}_{2} \rightarrow A + A + h\nu$
Penning effect:	$A^{*} + B \rightarrow A + B^{+} + e \quad [E_I(B) < E_x(A)]$

Threshold Voltage V_T

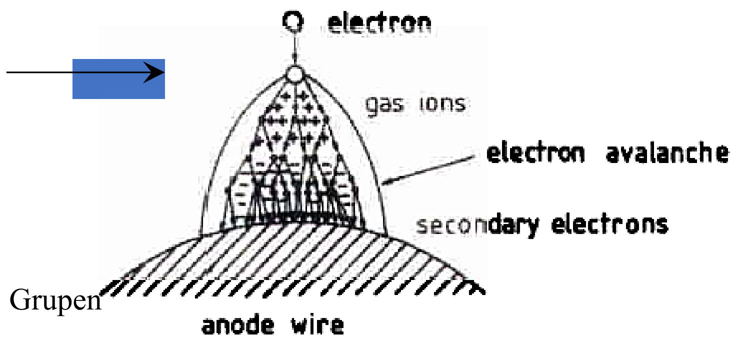

$\lambda_{m.f.p.} \sim few\ \mu m$

Example: Avalanche starts at $\sim 10^4 V / cm$

$50 - 100 \mu m$ from wire

$10 \mu m$ dia. wire at 1-2 kV

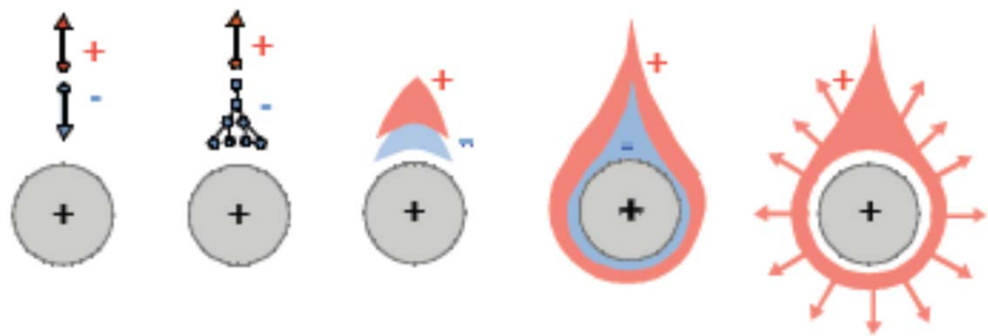

Avalanche Multiplication

Gain Factor

$\#e^- / \text{ion pairs} / cm \equiv 1^{st}$ *Townsend coefficient* $\equiv \alpha$

$$\alpha = \sigma_{ion} \frac{N_A}{V_{mol}}$$

$$where\ V_{mol} = 22.4\ l/mol\ \ (ideal\ gas); N_A\ :\text{Avigadro}$$

N(x)= no. electrons at x

$$dN(x) = \alpha N(x)dx \rightarrow \boxed{N(x) = N_0 e^{\alpha x}} = N_0 e^{\int_{r_k}^{r_i} \alpha(x)dx}$$

There is field dependance of α(x).

* 75-100 eV needed for high ionization probability.

1^{st} *Townsend coefficient* $\equiv \alpha / P$

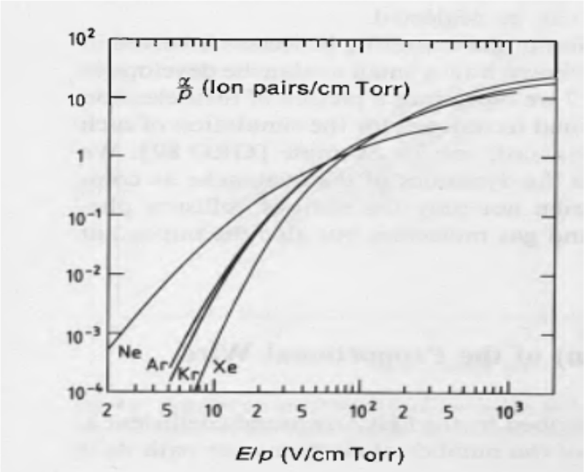

Blum & Rolandi

Process of amplification takes a few ns and occurs very close to wire.

$$w = 5 \text{ cm}/\mu\text{s} \qquad n\lambda \sim 50\ \mu\text{m}$$

$$\frac{50\text{x}10^{-4}\text{ cm}}{5\text{ cm}/\mu\text{s}} \sim 1\text{ ns}$$

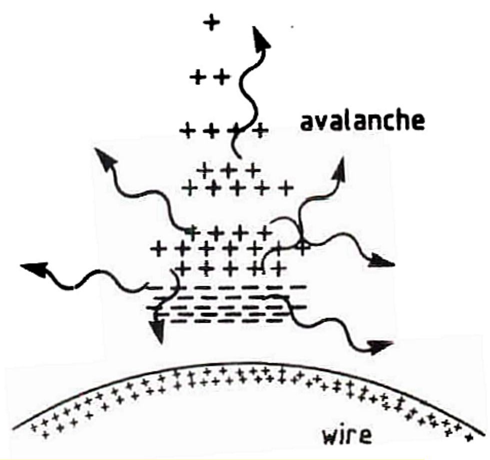

Detected signal:

- •Negative on anode
- •Positive on cathode

•A consequence of ΔE due to charge movement – mainly ions

Proportional chamber signal is due to motion of positive ions!

Ions dominate! Electron signal ~1 %.

Signal Time Dependence

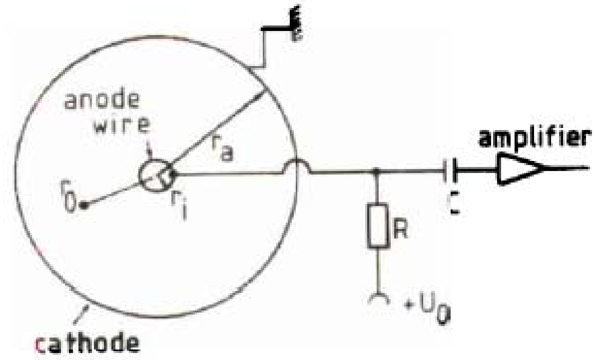

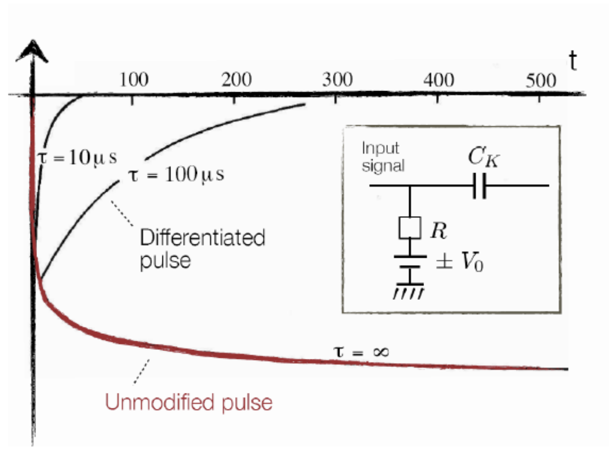

$$V(t) = -\frac{q}{4\pi\varepsilon_0 l}\ln\left(1+\frac{t}{t_0}\right)$$

$$\text{where } t_0 = \frac{\pi\varepsilon_0 r_i^2}{\mu C V_0}$$

Typically, after 10^{-3} of maximum drift time T, 50% of signal is reached.

$$v_{drift} = \mu E(r)$$

$$\mu = Mobility$$

l = cylinder length

Capacitance/unit length

$$C = \frac{2\pi\varepsilon_0}{\ln\frac{r_a}{r_i}}$$

Gas amplification factor

Ionization mode:

full charge collection
no multiplication; gain ≈ 1

Proportional mode:

multiplication of ionization
signal proportional to ionization
measurement of dE/dx
secondary avalanches need quenching;
gain ≈ $10^4 - 10^5$

Limited proportional mode:

[saturated, streamer]

strong photoemission
requires strong quenchers or pulsed HV;
gain ≈ 10^{10}

Geiger mode:

massive photoemission;
full length of the anode wire affected;
discharge stopped by HV cut

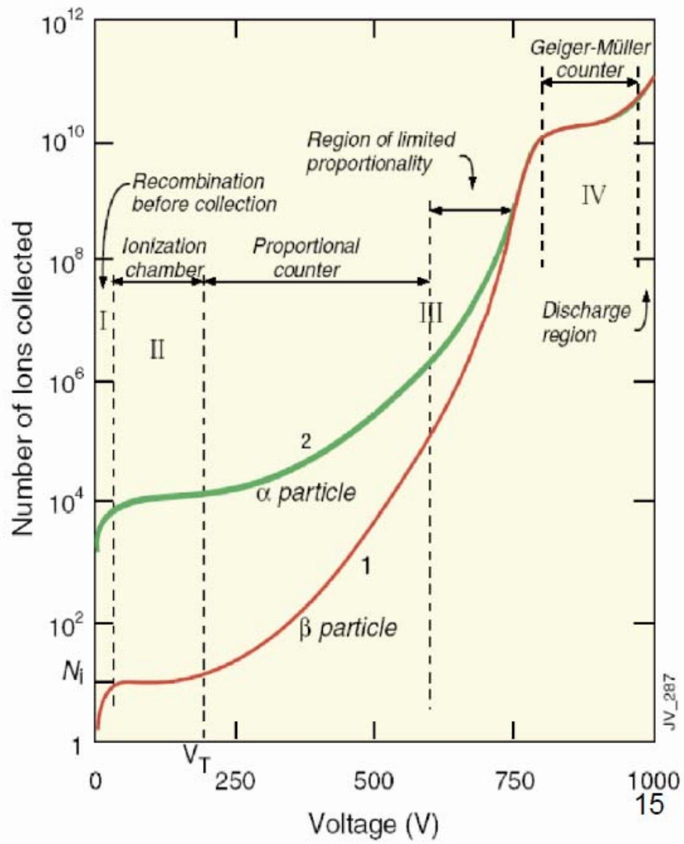

Geiger Counters

Transverse propagation of discharge.

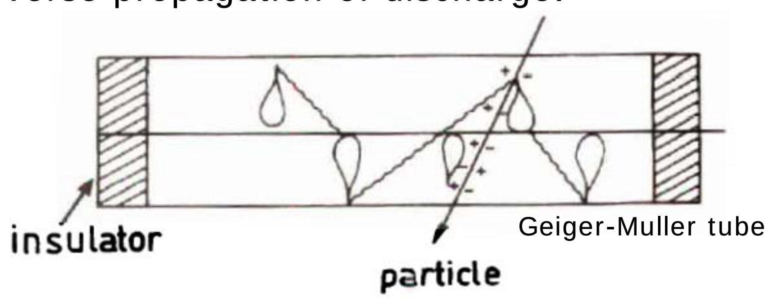

Schematic representation of the transverse avalanche propagation ıe anode wire in a Geiger counter.

$Q \propto$ Voltage

$\sim 10^{8\text{-}10} e^-$/primary

Typical 30μm diameter anode.

Gas ~Ar/X_{quench} 90/10

High fields →Avalanche →photons →P.E. effect → Avalanches propagate → (back to Avalanche)

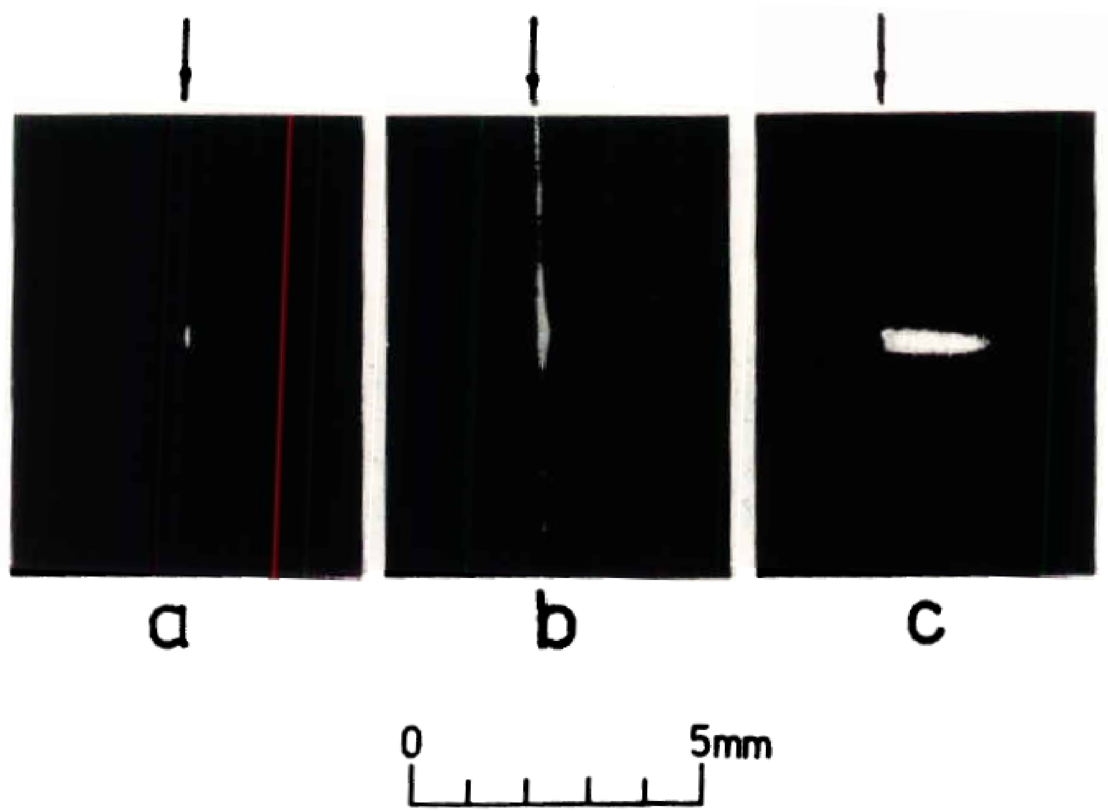

Fig. 4.17. Gas discharges in (a) a proportional counter, (b) a Geiger counter, and (c) a self-quenching streamer tube; the arrows indicate the position of the anode wire [166].

Grupen

Resistive Plate Chambers (RPC)

- **How it works**
  1. **Primary ionisation**
  2. **Avalanche**
  3. **Surfaces charged by electrons/ions**
  4. **Charges on electrodes are annihilated with some time constant τ**

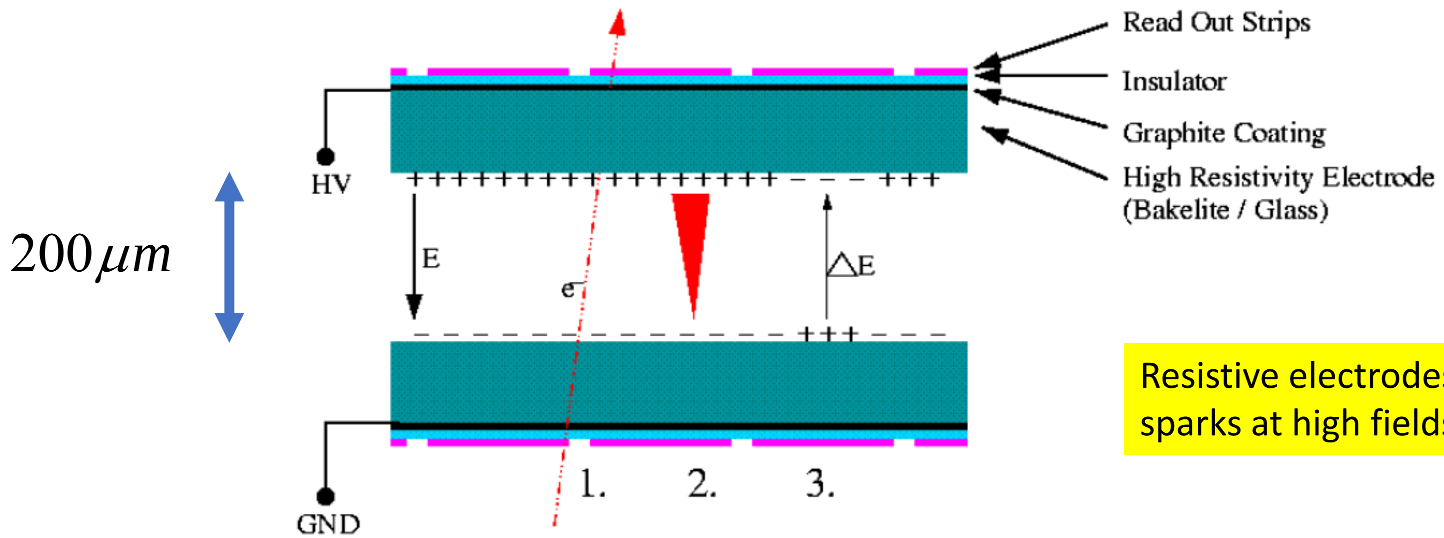

Resistive electrodes prevent sparks at high fields

Ref: Christian Lippmann (GSI) *https://web-docs.gsi.de/~lippmann/files/presentations/gsi-2002.pdf*

RPC Applications: trigger, timing

- Large areas (low cost/m^2)
- Low rates ($\lesssim$1 kHz/cm^2)
- Good timing (<500 ps; 30-80 ps for 200μm gap)
- "Easy" construction – industrial methods

Used by ATLAS at LHC

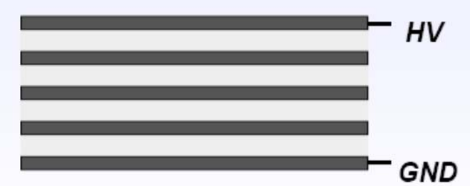

Multigap RPC - exceptional time resolution suited for the trigger applications

A. Akindinov et al., NIM A456(2000)16

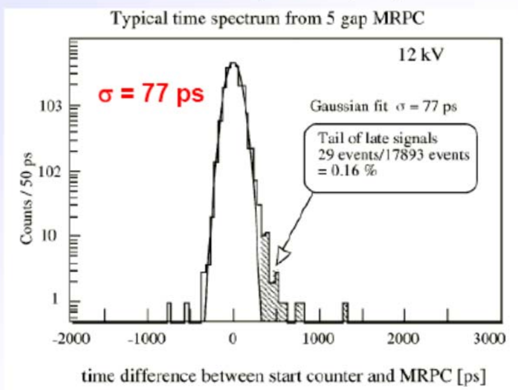

Time resolution

Multiwire Proportion Chambers (MWPC)

G. Charpak et al, Nucl. Instr. and Meth. 62(1968)235

The Nobel Prize in Physics 1992

The Royal Swedish Academy of Sciences awards the 1992 Nobel Prize in Physics to **Georges Charpak** for his invention and development of particle detectors, in particular the multiwire proportional chamber.

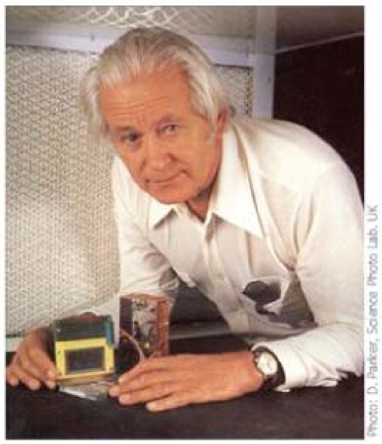

Georges Charpak
CERN, Geneva, Switzerland

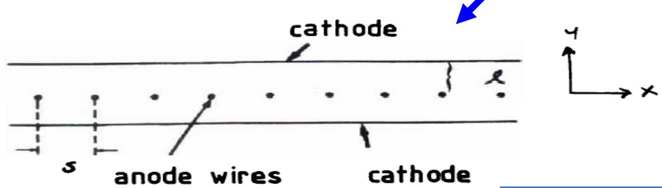

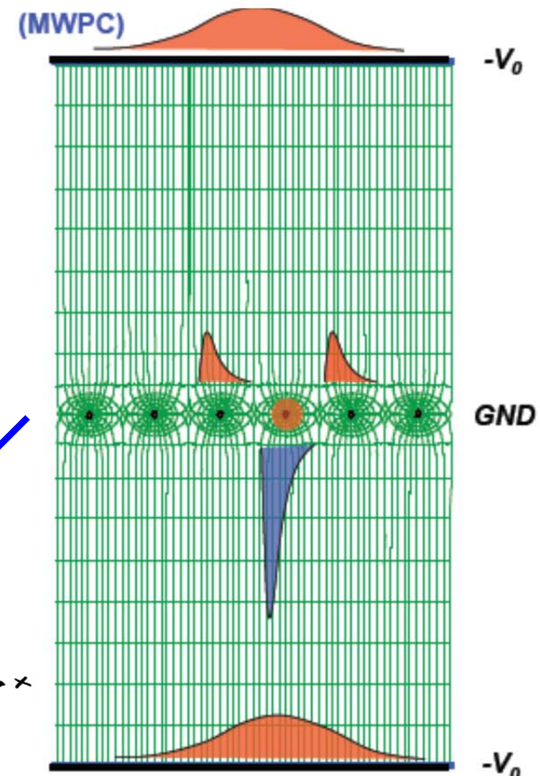

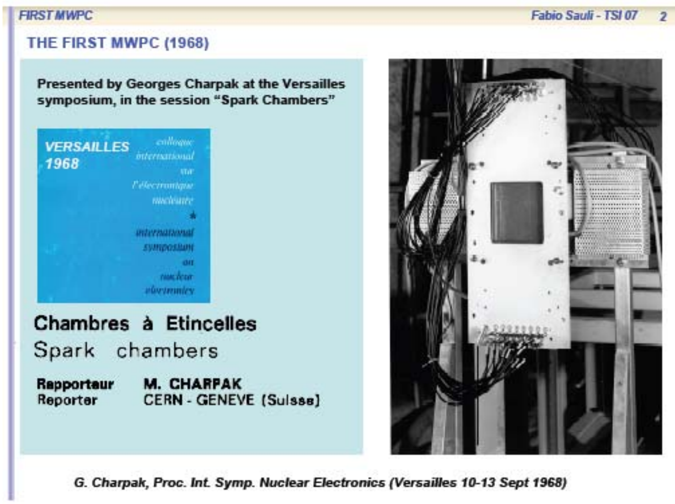

20 µm Ø Au-plated tungsten wires soldered to printed circuit board:

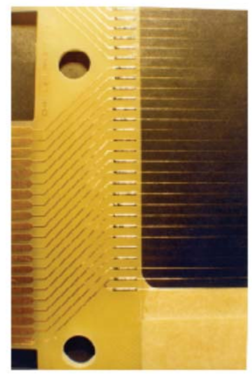

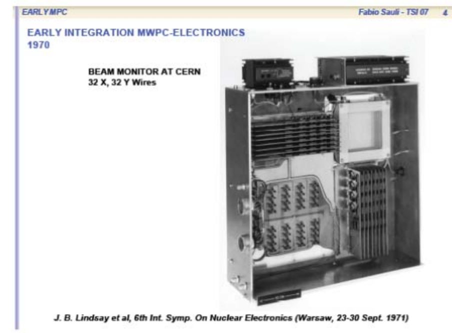

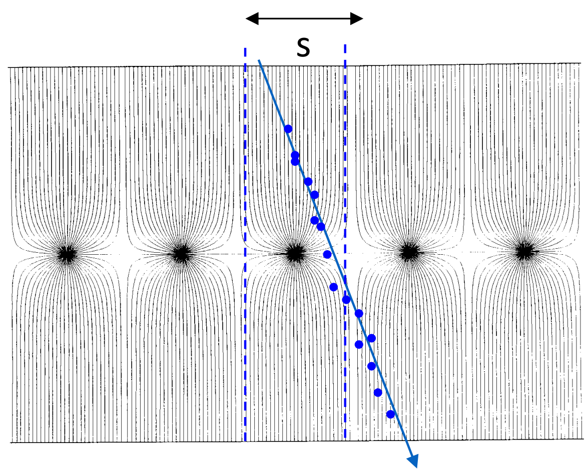

Normally digital readout:
spatial resolution limited to

$$\sigma_x \approx \frac{s}{\sqrt{12}}$$

Modern MWPCs: ATLAS Thin Gap Chambers

https://arxiv.org/abs/1509.06329

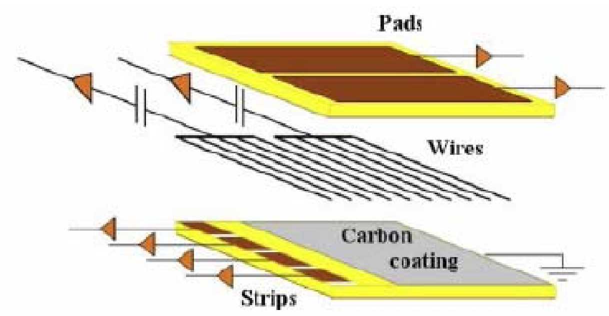

Figure 2: Schematic diagram of the basic sTGC structure.

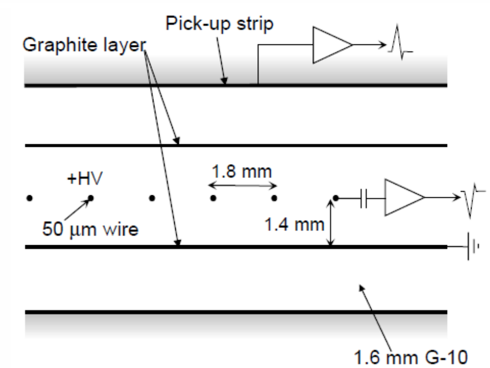

Wires 50μm dia. gold plated W

Pitch: 1.8 mm

Anode-Cathode dist.: 1.4 mm

Cu strips: 3.2 mm pitch

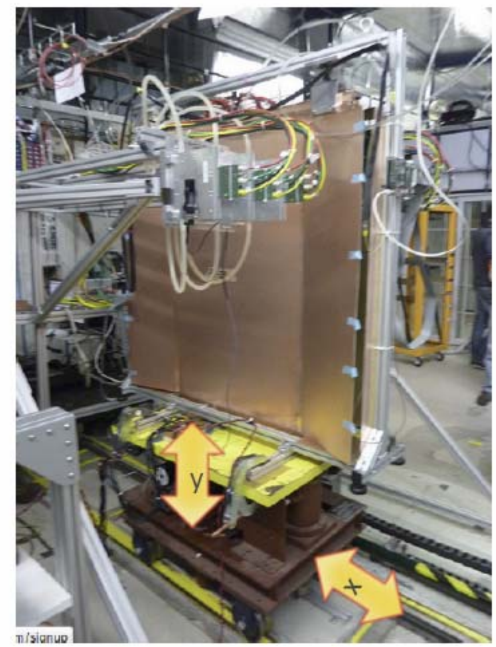

4. Drift Chambers

Precision in MWPCs is limited by wire spacing

- Low field region between wires in MWPC

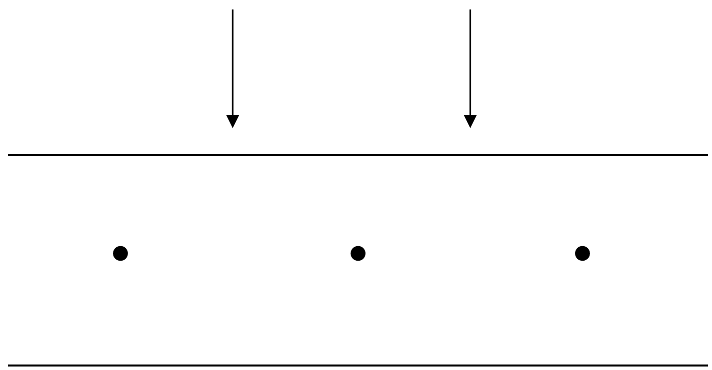

- Variable drift velocity w(E)

Try to find a better geometry where drift velocity *w*=constant so

$$x = \int_{t_0}^{t_1} w\,dt = w\Delta t$$

e.g.

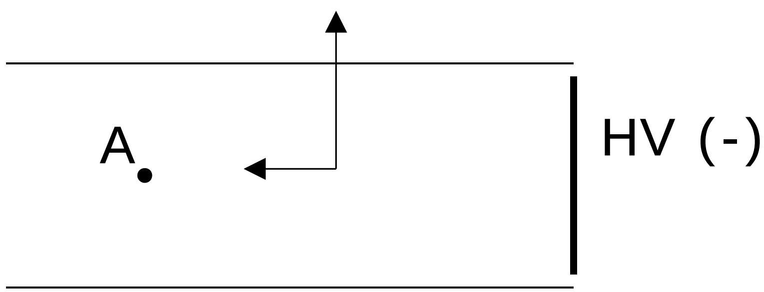

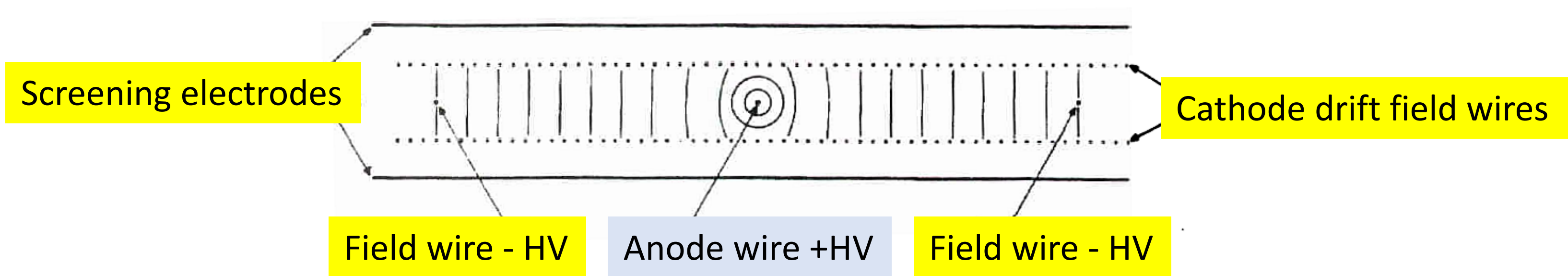

Figure 27 **Principle of construction of the high-precision drift chamber (60).**

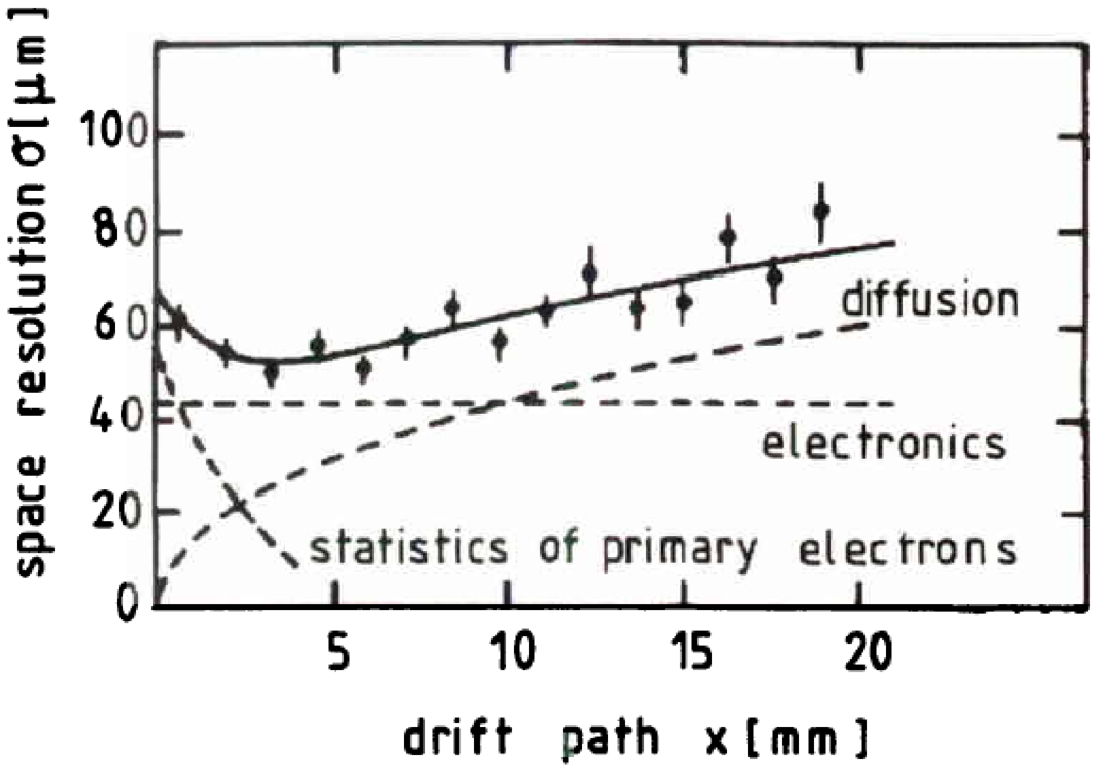

Grupen

$\sigma_{ave} \approx 70\mu m$

Spatial resolution of a drift chamber as a function of drift path

Construct Drift Chamber Cells from Wires or tubes

Drift Chambers – 3D Track Coordinates

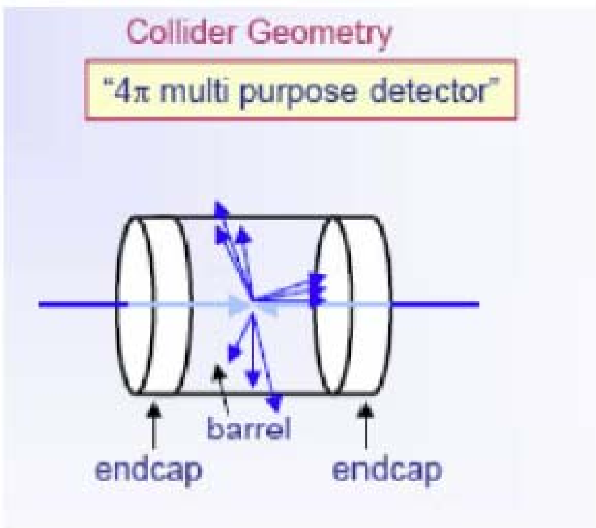

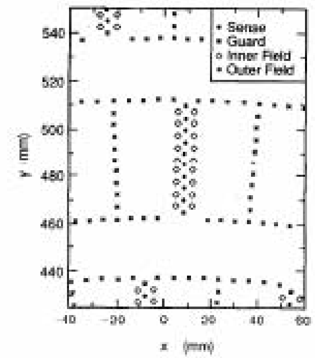

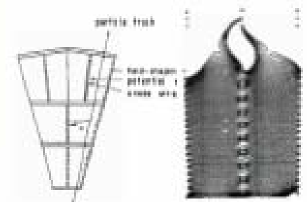

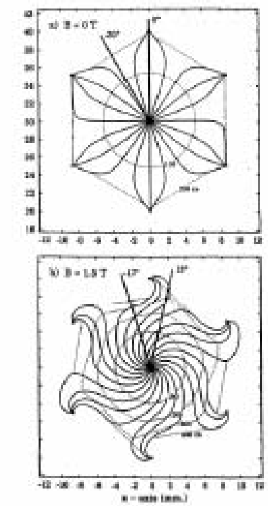

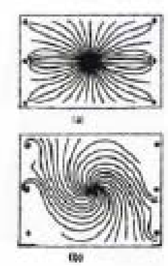

Drift cell gives 2D information

Straws

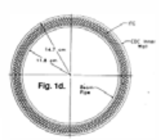

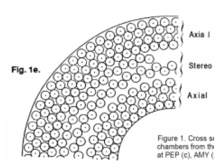

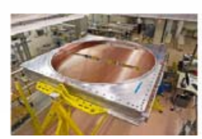

Straw Tubes

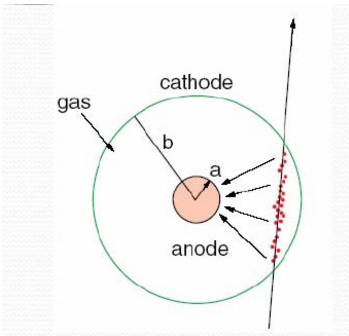

Track Reconstruction

Straw Tube Array

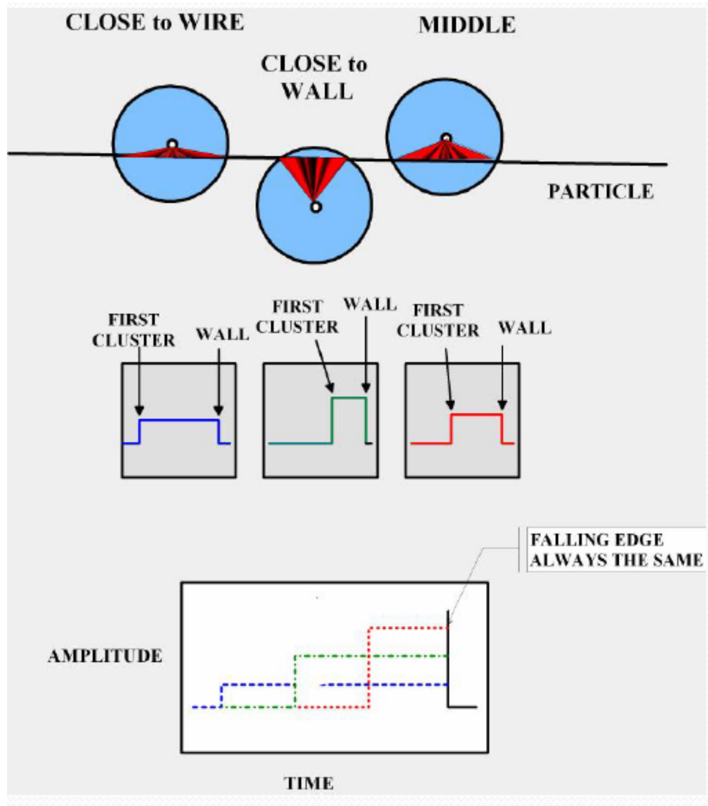

Leading edge gives the arrival time of the first cluster

Straw Tubes

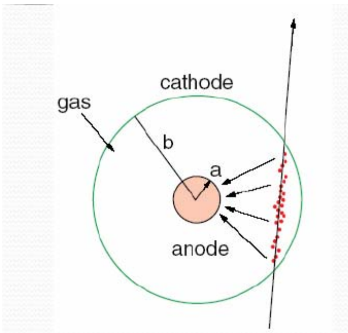

NA62

ATLAS TRT

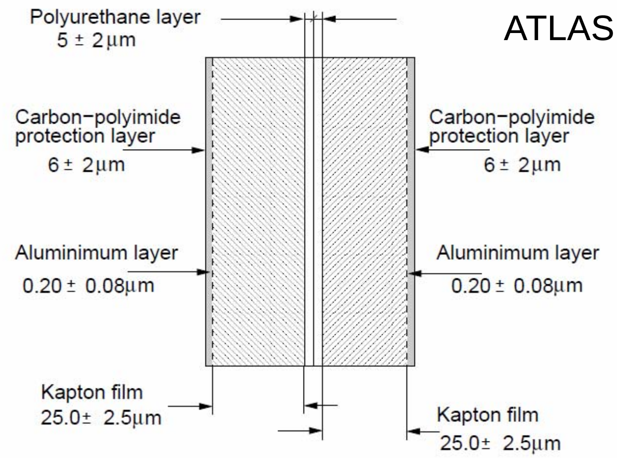

Figure 1. The TRT straw wall design.

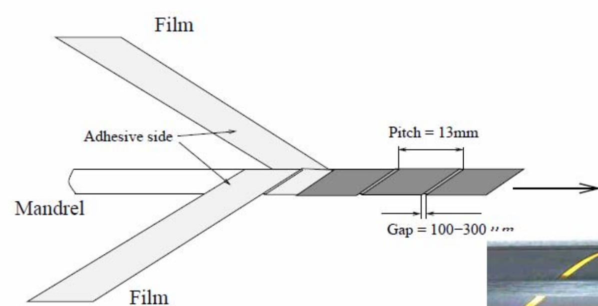

Figure 2. Schematic view of straw manufacturing process.

ATLAS TRT: http://iopscience.iop.org/article/10.1088/1748-0221/3/02/P02013/meta

MWPC and Drift Chambers: Second coordinate measurements

Crossed wire planes. Ghost hits. Restricted to low multiplicities. Also stereo planes (crossing under small angle).

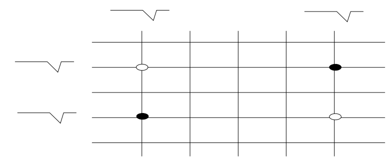

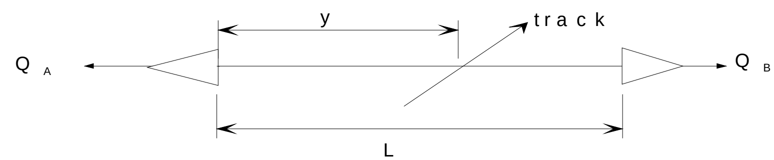

Charge division. Resistive wires (Carbon,2kΩ/m).

Typically σ~1% L

$$\frac{y}{L} = \frac{Q_B}{Q_A + Q_B} \qquad \sigma\left(\frac{y}{L}\right) \text{ up to } 0.4\%$$

Timing difference

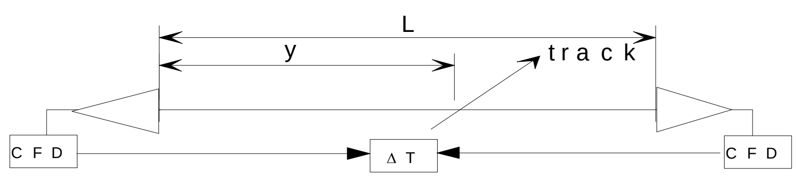

$$\sigma(\Delta T) = 100\,ps$$
$$\rightarrow \sigma(y) \approx 4\,cm$$

Stereo Wires:

$$\sigma_{\Delta Z} \sim \frac{\sigma_{r\phi}}{\sin\gamma}$$

$$\sim \frac{200\,\mu m}{\sin(4°)}$$

$$\sim 3mm$$

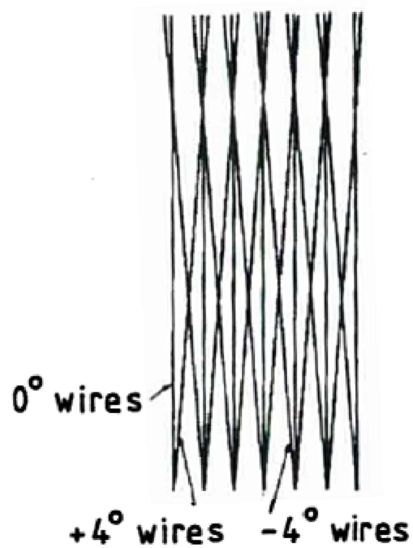

Grupen

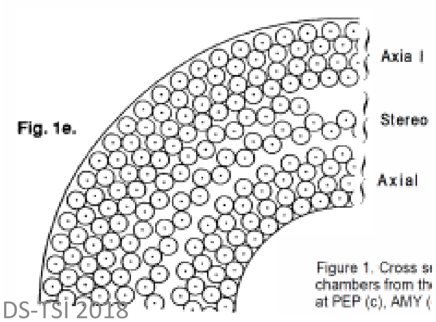

2nd Coordinate Measurement

Induced signals on Cathode strips/pads

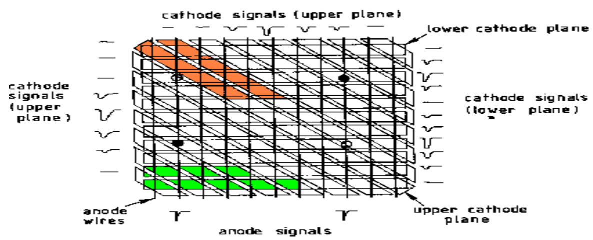

Analog readout of cathode planes.
$\rightarrow \sigma \approx 100\ \mu m$

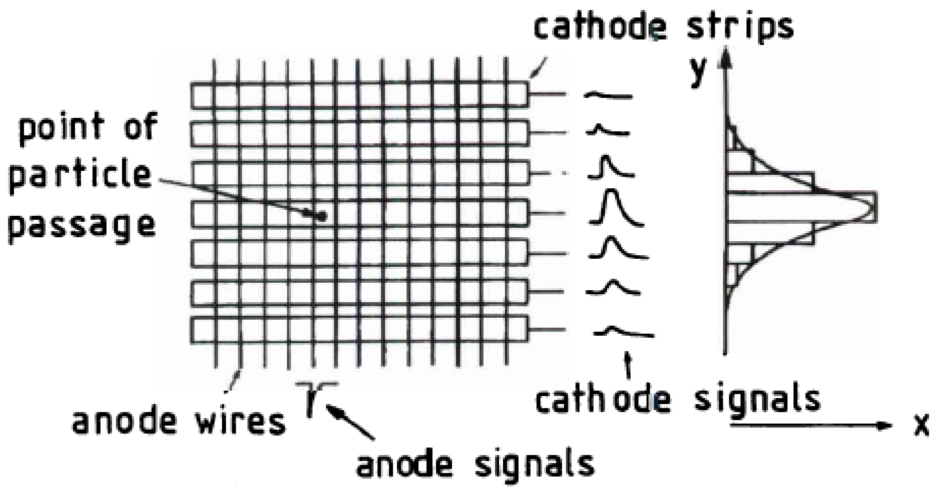

Fig. 4.28. Illustration of the cathode readout in a multiwire proportional chamber.

Center of Gravity Method:
(Biases depending on number of strips hit.)

Grupen

X-Y Readout in a MWPC: Cathode strips

Charge induced on strips near the wire

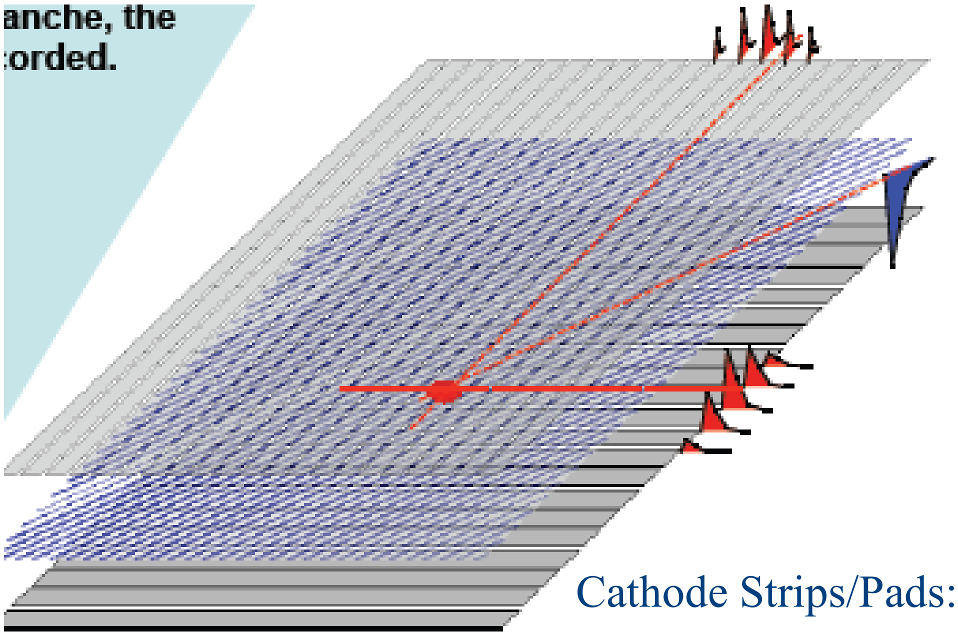

$\sigma_Z \sim 20 - 50 \mu m$ achieved

G. Charpak and F. Sauli, Nucl. Instr. and Methods 113(1973)381

Modern MWPCs: ATLAS Thin Gap Chambers

https://arxiv.org/abs/1509.06329

Wires 50μm dia. gold plated W

Pitch: 1.8 mm

Anode-Cathode dist.: 1.4 mm

Cu strips: 3.2 mm pitch

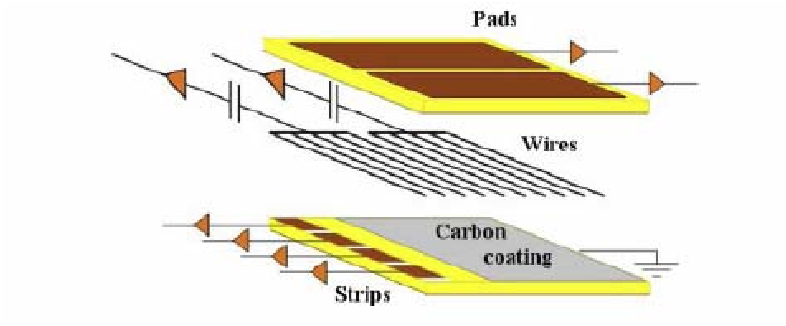

Figure 2: Schematic diagram of the basic sTGC structure.

Center of gravity

Bias-corrected

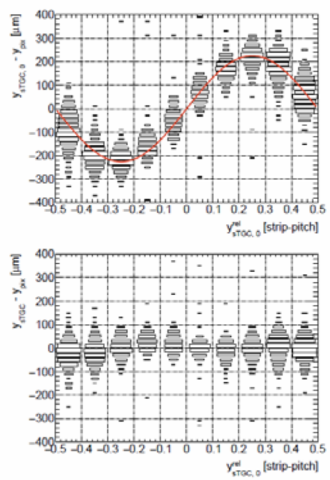

Figure 6: The differential non-linearity for sTGC strip-clusters is shown before (top) and after the sinusoidal correction is applied (bottom).

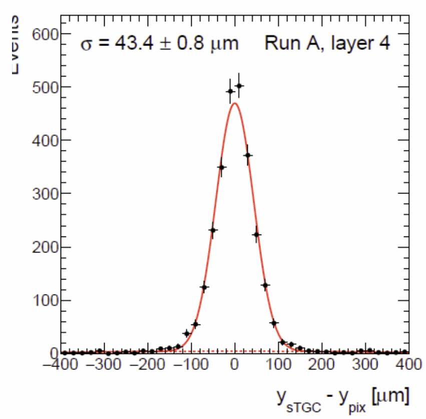

Time Projection Chamber (TPC) 3-D Tracking

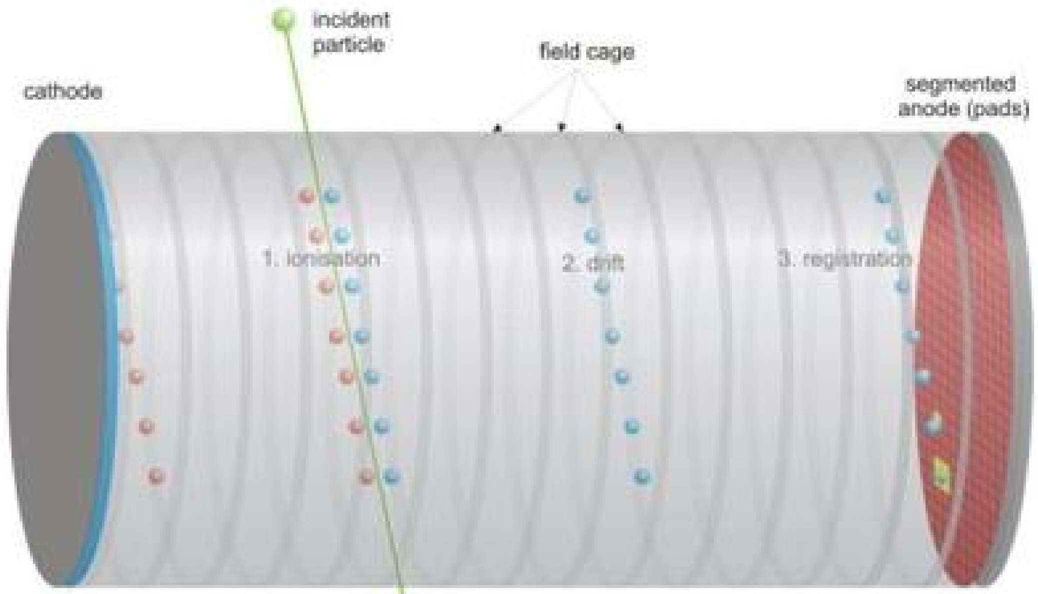

(O. Schäfer, LC)

z

E

B

Track Segment localization:
Anode Amplification Region
(2 coordinates e.g. x,y)
MWPC+ pads, strips,
GEM + pads, strips,
Micromegas + pads, strips,
...

Drift Time: 3rd Coordinate (z)
External trigger time reference

Typical Resolutions:
x,y ~200 µm
z ~mm

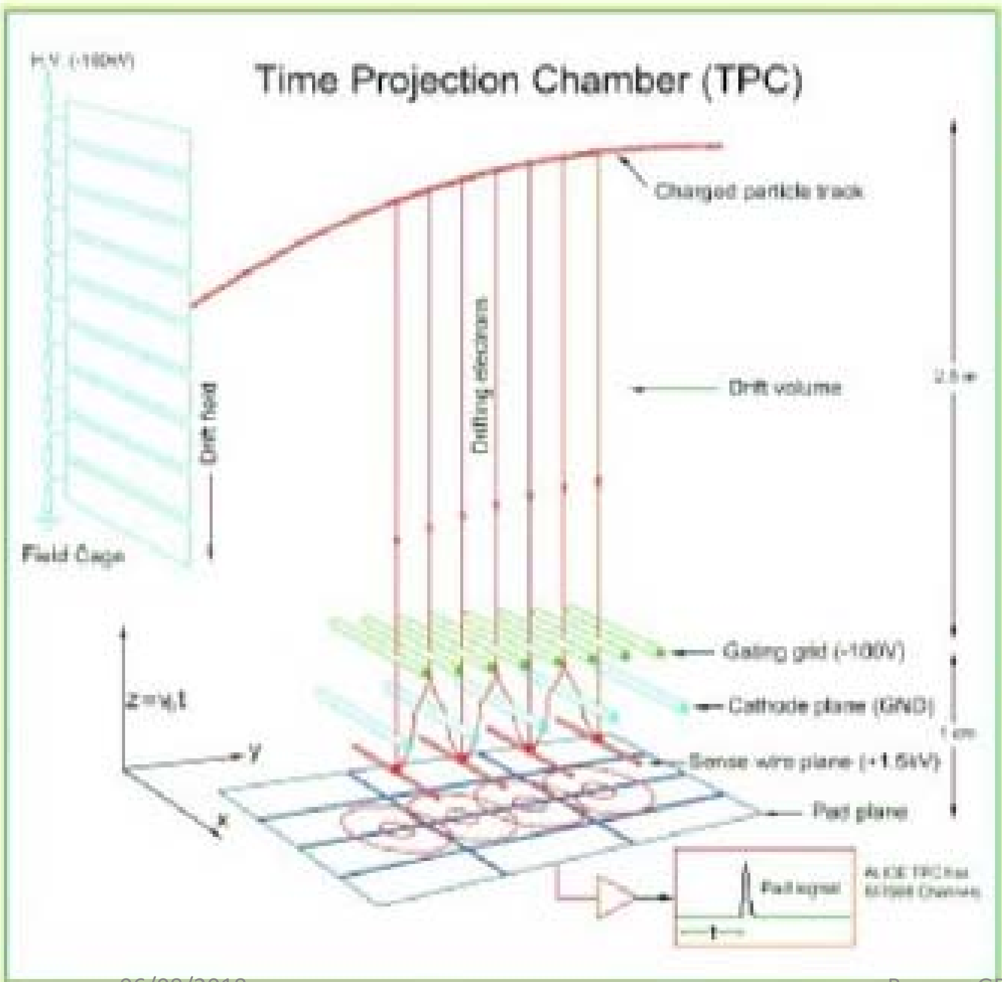

TPC Advantages

- 3D track information – track containment
- Limited readout area/channels needed
- Good dE/dx resolution (5-10%)
- Suppressed transverse diffusion
- Moderate, low mass – limits MCS

TPC Challenges

- Long drift times – limits rate capability
- Large volume – limits precision
- High voltages – breakdowns
- High data volume
- Ion feed back issues (gating grids)

Dave Nygren (1976)

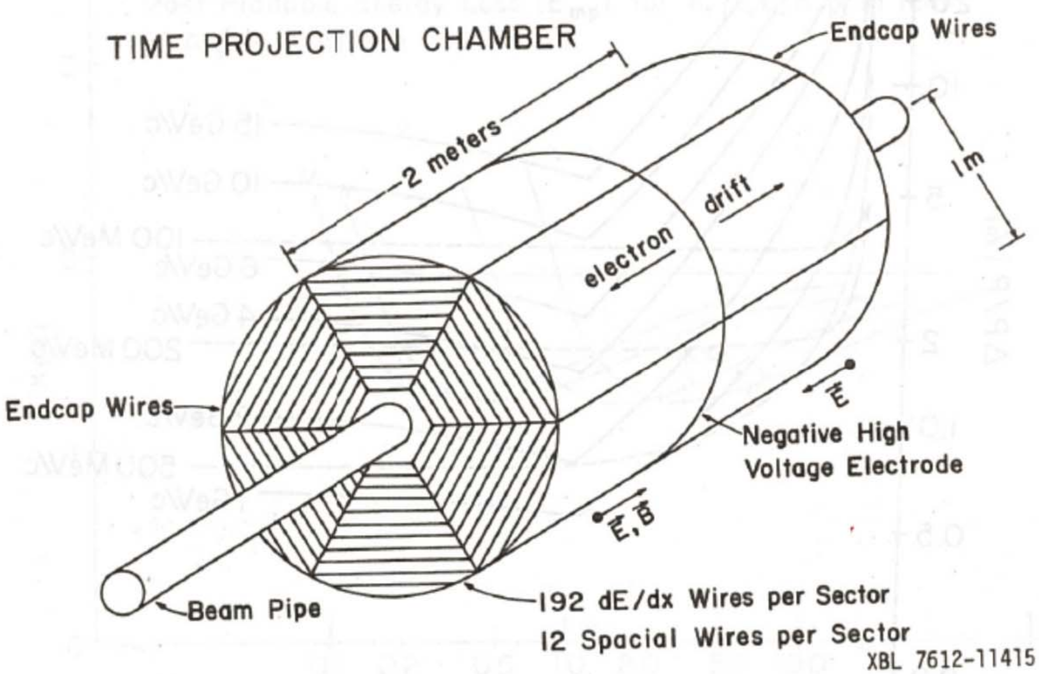

Fig. IIIA.2

TRIUMF TPC (1980)

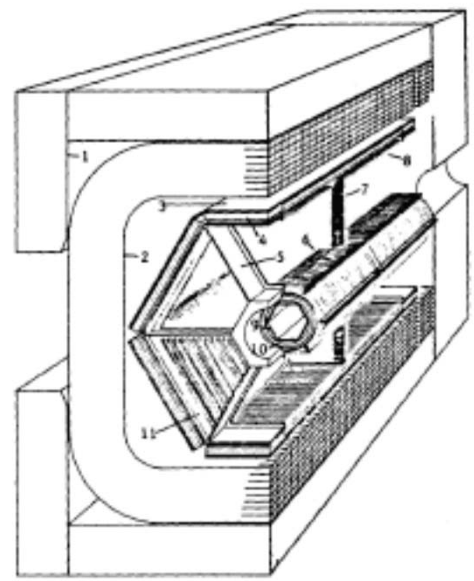

0.85 T

TRIUMF TPC

Suppression of diffusion

Position resolution vs drift distance

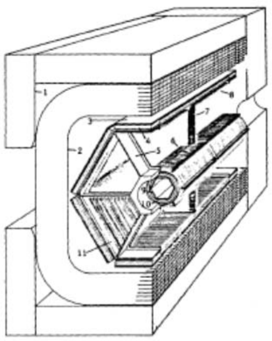

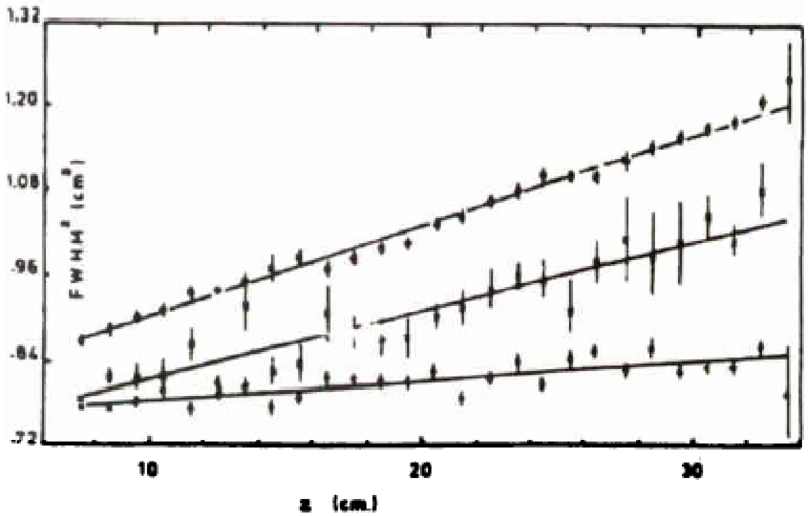

$$\sigma^2_{PRF}(l_D) = \sigma^2_0 + \sigma^2_D(l_D)$$

Lohse/W

Figure 31: *Squared FWHM of the PRF as function of the drift distance (called "z" in the figure) for different magnetic fields as determined from cosmic ray tracks [22]. The upper data points are for B = 0 kG, the middle ones for B = 2.3 kG and the lower ones for B = 8.5 kG [22].*

SEE: The Time Projection Chamber, J.A. Macdonald ed. (AIP Conf. Proc. 108, 1984)

STAR TPC AT RHIC

RELATIVISTIC HEAVY ION COLLISIONS AT ENERGY UP TO 100GeV/nucleon

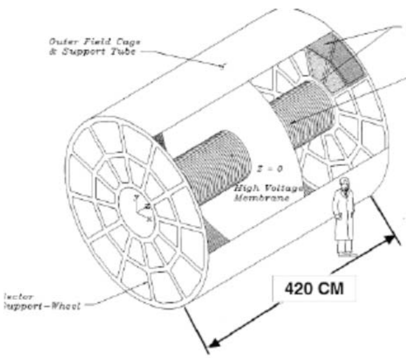

TPC: 2x210 cm long, 4 m Ø
Magnet: 0.5 T
P10 gas filling (Ar-CH_4 90-10)
136,000 pads readout
Gating wire grid

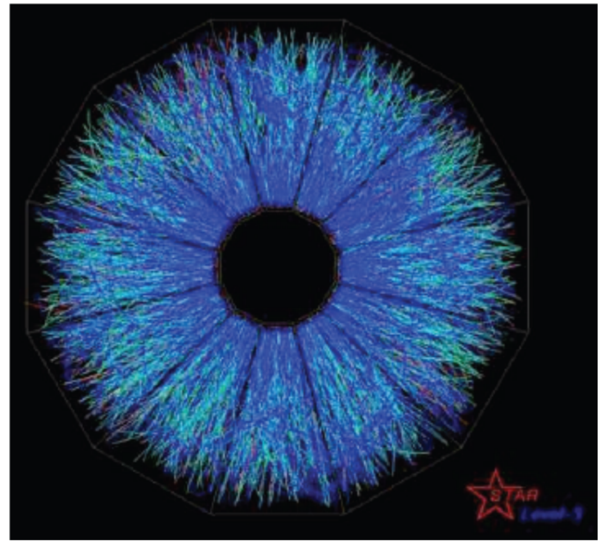

M. Anderson et al, Nucl. Instr. and Meth. A499(2003)659

ALICE TPC up and running

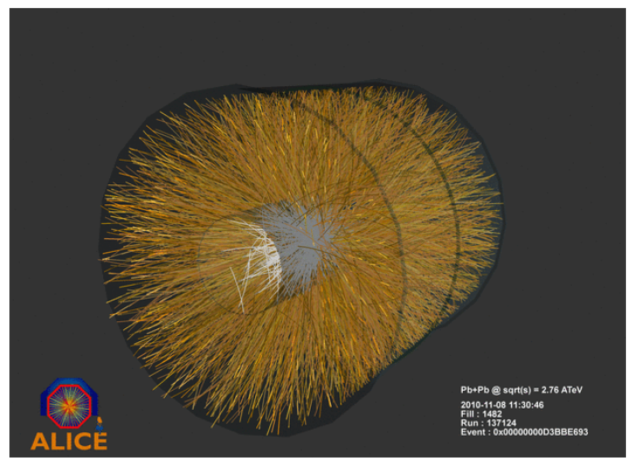

CERN ALICE TPC

95 m^3 largest TPC ever built

Particle ID using dE/dx

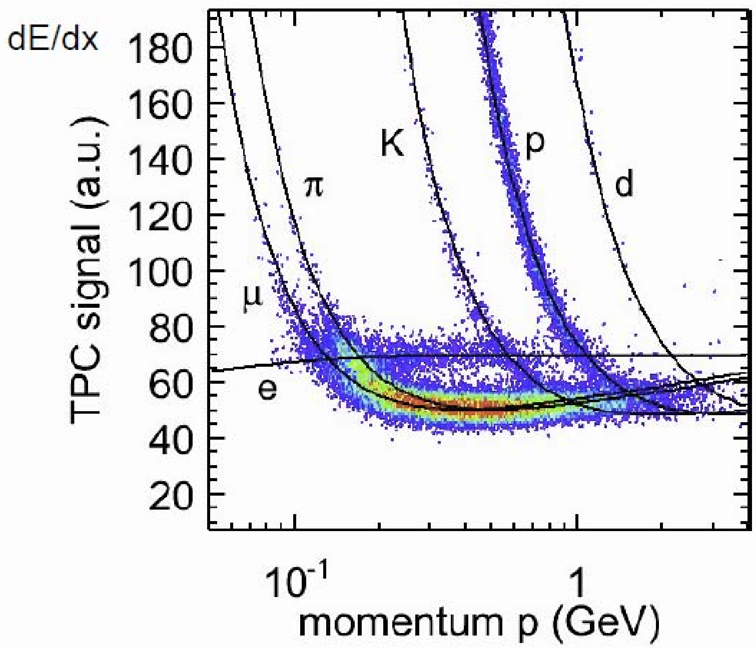

The energy loss as a function of momentum p=mcβγ is dependent on the particle mass

By measuring the particle momentum (deflection in a magnetic field) and the energy loss one gets the mass of the particle, i.e. particle ID

(at least in a certain energy region)

Fluctuations in dE/dx for thin absorbers (e.g. gases) are important: Landau distribution.

With a large number of measurements, the truncated mean energy loss gives best results.

5. Microstrip Gas Chambers

A. Oed (1988).

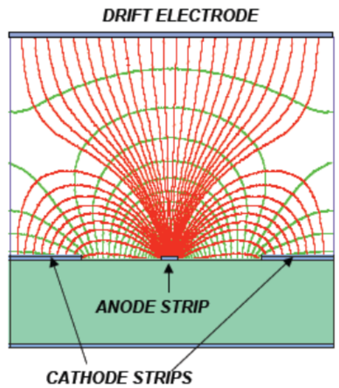

A.Oed, Nucl. Instr. and Meth. A263(1988)351

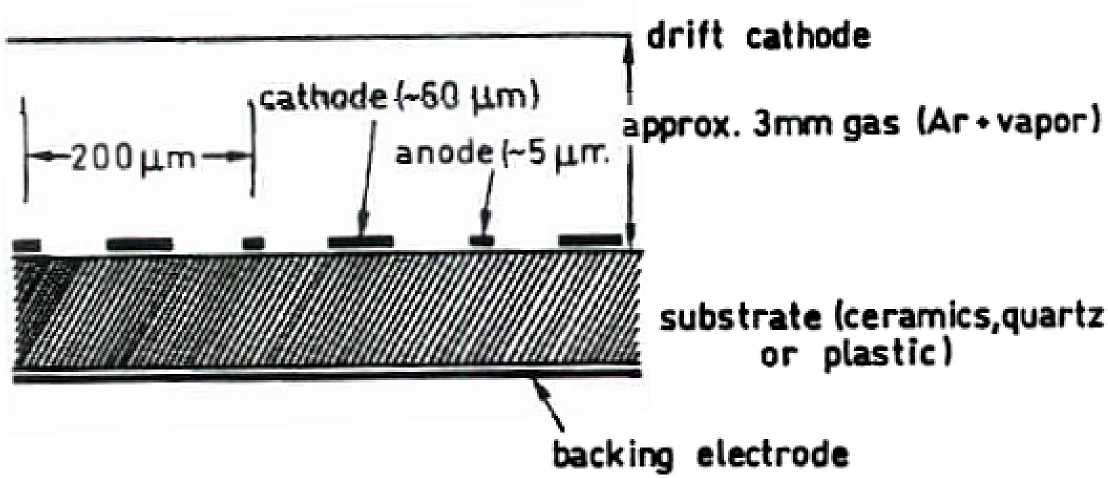

Fig. 4.30. Schematic arrangement of a microstrip gas detector.

Grupen

Micromegas

Thin gap parallel plate avalanche chamber

Charpak and Giomatraris (1996)

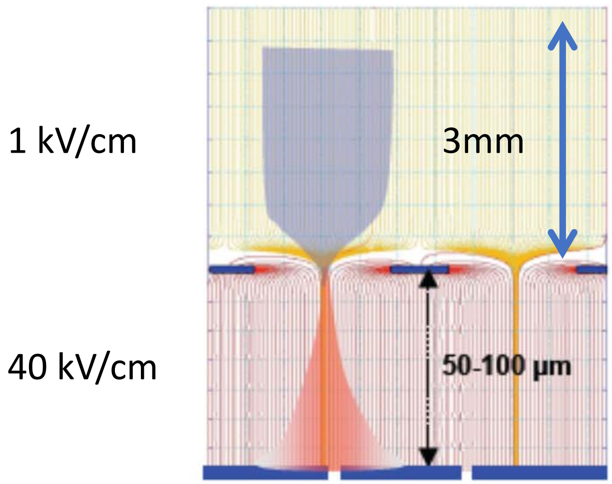

Y. Giomataris et al, Nucl. Instr. and Meth. A376(1996)29

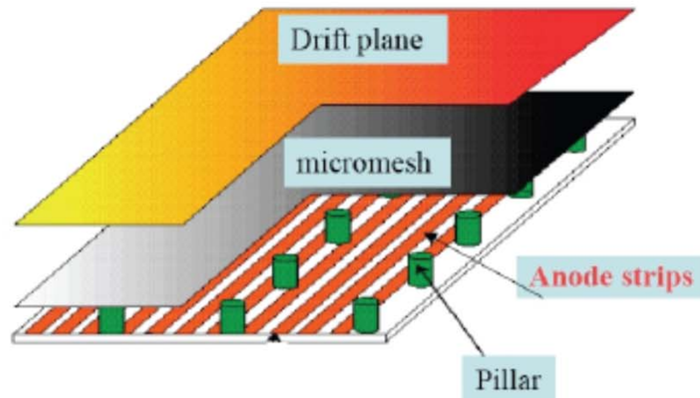

Y. Giomataris, Nucl. Instr. Aand Meth. A419(1998)239

MICROMEGAS PERFORMANCES

FAST ELECTRON SIGNALS WITH SLOW ION TAIL:

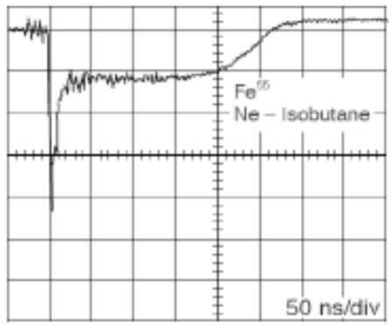

GAP DEPENDENCE OF FAST SIGNAL:

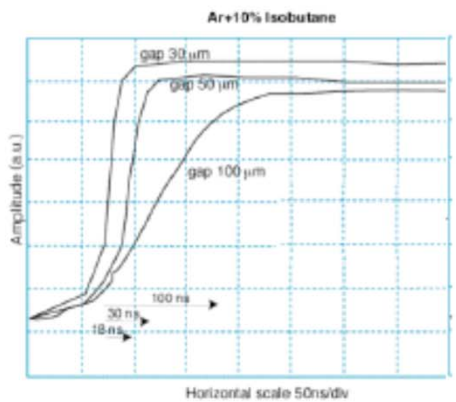

A. Bay et al,
Nucl. Instr. and Meth. A488(2002)162

CLUSTER SIZE (LOW SPREAD GAS):

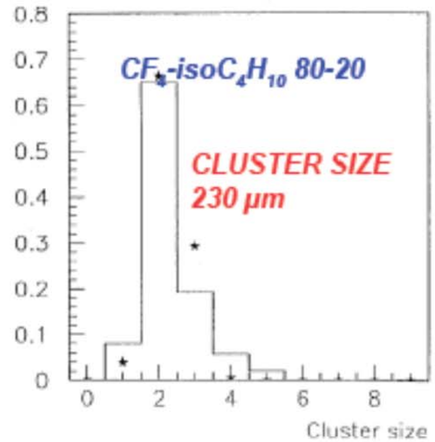

POSITION ACCURACY (100 µm PITCH STRIPS)

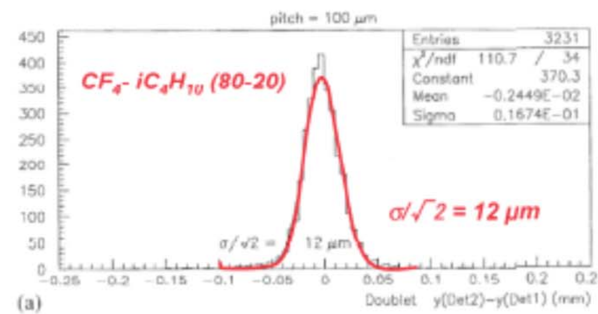

J. Derré et al,
Nucl. Instr. and Meth. A459(2001)523

Micromegas: Good energy and time resolutions.

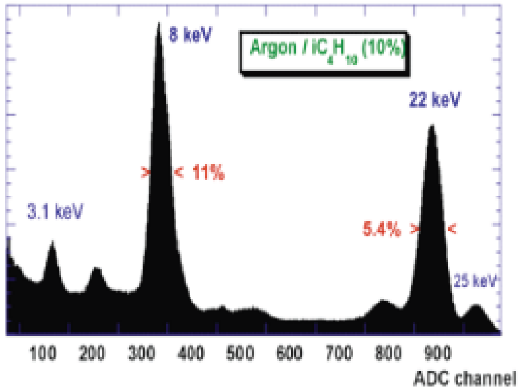

A. Delbart et al,
Nucl. Instr. and Meth. A461(2001)84

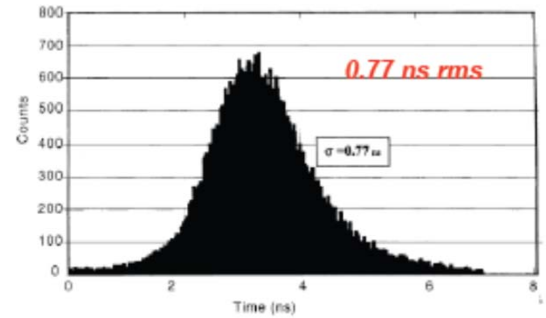

J. Derré et al, Nucl. Instr. And Meth. A449(2000)314

MICROMEGAS TPC PROTOTYPE FOR T2K

2 MICROMEGAS (26x27 cm²) ON FLANGE

READOUT: 8x8 mm² PAD PLANE

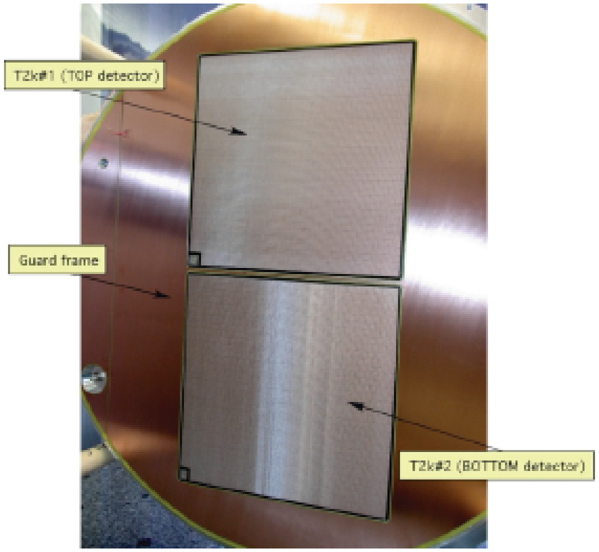

CERN TEST BEAM TRACKS:

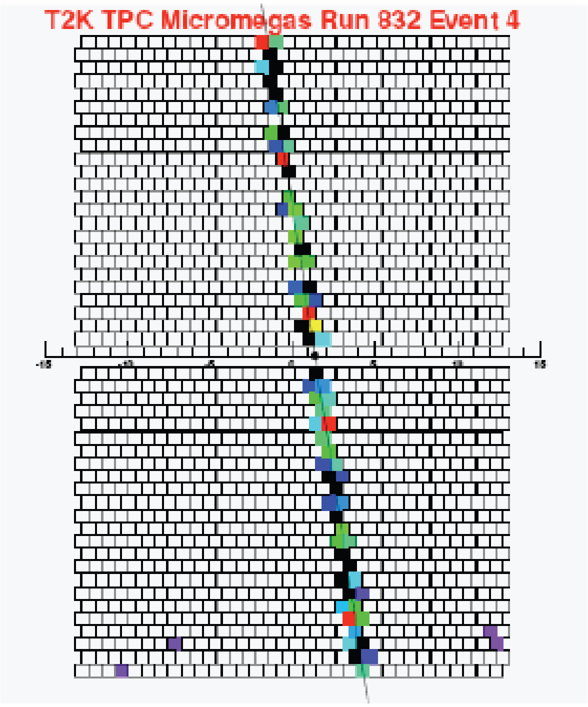

R. De Oliveira et al,
A Micromegas based TPC for the T2K ND280m detector(2006)

Nuclear Instruments and Methods in Physics Research A 386 (1997) 531–534

NUCLEAR INSTRUMENTS & METHODS IN PHYSICS RESEARCH Section A

ELSEVIER

Letter to the Editor

GEM: A new concept for electron amplification in gas detectors

F. Sauli

CERN, CH-1211 Genève, Switzerland

Received 6 November 1996

Abstract

We introduce the gas electrons multiplier (GEM), a composite grid consisting of two metal layers separated by a thin insulator, etched with a regular matrix of open channels. A GEM grid with the electrodes kept at a suitable difference of potential, inserted in a gas detector on the path of drifting electrons, allows to pre-amplify the charge drifting through the channels. Coupled to other devices, multiwire or microstrip chambers, it permits to obtain higher gains, or to operate in less critical conditions. The separation of sensitive and detection volumes offers other advantages: a built-in delay, a strong suppression of photon feedback. Applications are foreseen in high rate tracking and Cherenkov Ring Imaging detectors. Multiple GEM grids assembled in the same gas volume allow to obtain large effective amplification factors in a succession of steps.

GEM

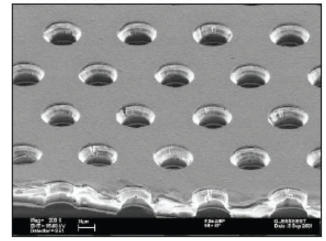

Typical geometry:
5 μm Cu on 50 μm Kapton
70 μm holes at 140 μm pitch

5-10,000 INDEPENDENT PROPORTIONAL COUNTERS per cm²

Max. fields ~40kV/cm
Gain ~100 - 1000

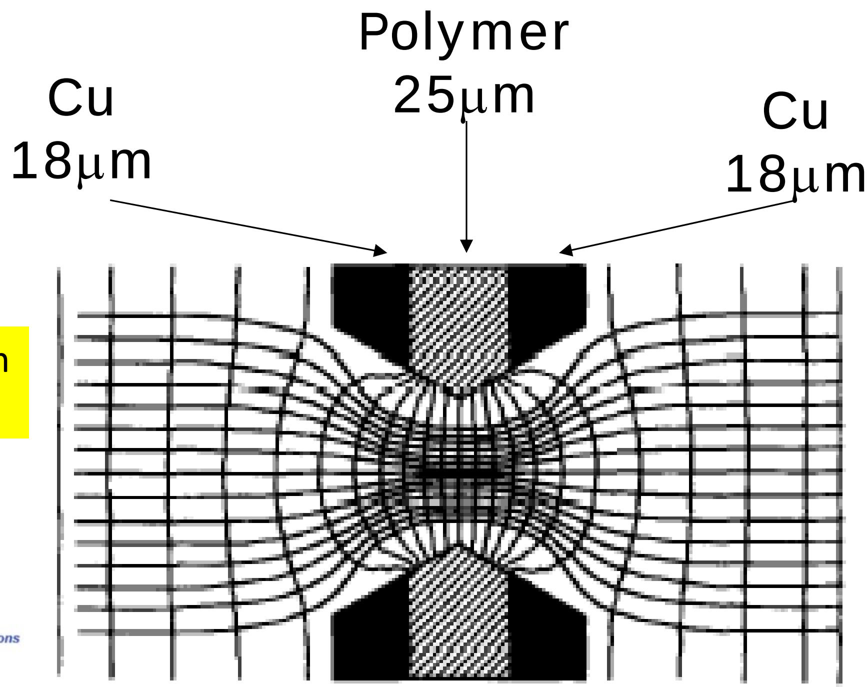

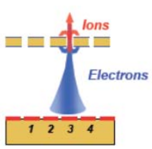

Fig. 2. Computed electric field in the multiplying channel. Only the central field lines have been plotted.

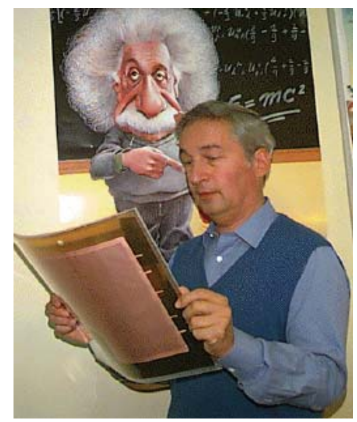

Fabio Sauli with a GEM

See “Tactic” TPC manual -- one of the GRIDS experiments uses a single GEM layer.

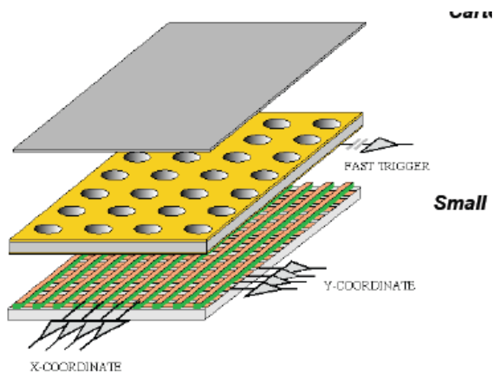

A. Bressan et al, Nucl. Instr. and Meth. A425(1999)254

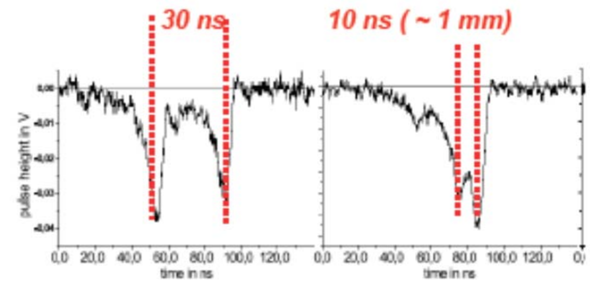

Good double pulse resolution possible.

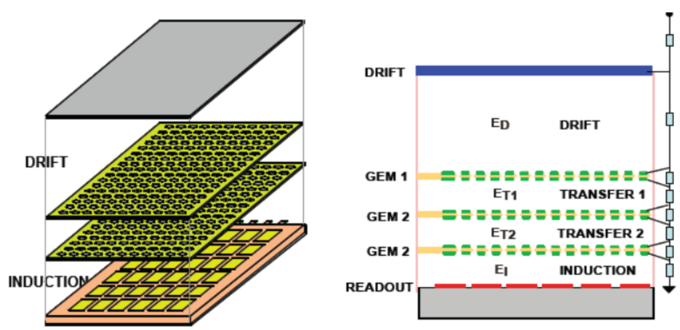

C. Büttner et al, Nucl. Instr. and Meth. A409(1998)79
S. Bachmann et al, Nucl. Instr. and Meth. A438(1999)376

Multiple GEM layer to increase the gain.

COMPASS GEM TRACKER

PERFORMANCES IN DATA TAKING CONDITIONS

UNIFORMITY OF EFFICIENCY:
~ 97% FOR MINIMUM IONIZING TRACKS, HIGH INTENSITY RUNS (2.5x10^4 Hz mm^{-2})

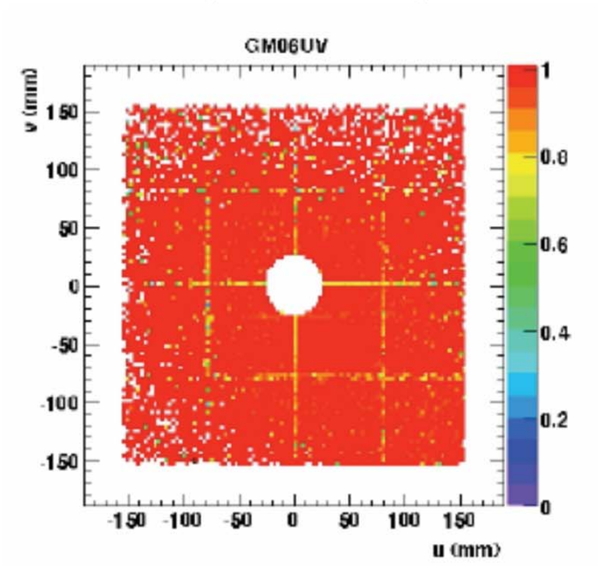

B. Ketzer et al, Nucl. Instr. and Metrh. A535(2004)314

POSITION ACCURACY

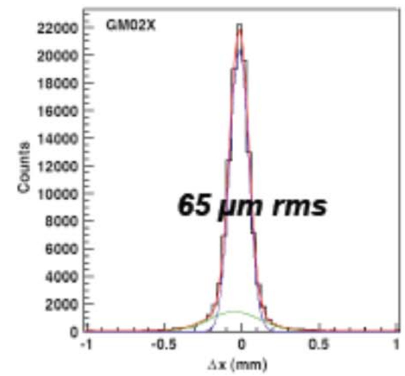

TIME RESOLUTION

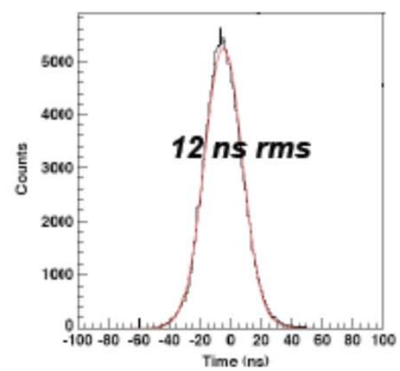

6. Summary: Gas Ionization Detectors

- Gas ionization detectors are found in myriad applications in particle and nuclear physics detectors
- Excellent choices for tracking, momentum measurements, particle identification, triggering, low energy x-ray measurements, dosimetry, …..
- Suitable for large and small scale applications requiring high precision localization at relatively low cost
- Among the GRIDS experiments is the ``Tactic`` TPC
  - GEM gain structure
  - Embedded α source
  - Possible measurements: MCS, dE/dx, range, Bragg peak…